WISCONSIN HIGHWAY RESEARCH PROGRAM #0092-03-12

DEVELOPMENT OF METHODOLOGY TO INCLUDE THE STRENGTH CONTRIBUTION OF SELECT SUGRADE MATERIALS IN PAVEMENT STRUCTURE

A FINAL REPORT on the WHRP Project

"Strength Contribution of Select Subgrade Reinforcement Materials"

Principal Investigators**:** Tuncer B. Edil and Craig H. Benson

Graduate Research Assistants: Woon-Hyung Kim and Burak F. Tanyu

Geo Engineering Program

Department of Civil and Environmental Engineering

University of Wisconsin-Madison

SUBMITTED TO THE WISCONSIN DEPARTMENT OF TRANSPORTATION

October 31, 2005

ACKNOWLEDGEMENT

Financial support for the study described in this paper was provided by the Wisconsin Department of Transportation (WisDOT) through the Wisconsin Highway Research Program (WHRP). Alliant Energy Corporation supplied the bottom ash, Grede Foundries Inc. supplied the foundry sand and foundry slag, and Yahara Materials supplied the Grade 2 granular backfill. Tenax Corporation and Amoco Fabrics and Fibers Co. supplied the geosynthetics. The LSME experiments were conducted in the University of Wisconsin Structures and Materials Testing Laboratory (SMTL). Professor Steven Cramer (Director of SMTL) and Mr. William Lang (Manager of SMTL) provided valuable assistance during the LSME tests. The conclusions and recommendations in this report are solely those of the authors, and do not necessarily reflect the opinions or policies of WisDOT, WHRP, the material suppliers, or others who provided assistance during the study. Endorsement by persons other than the authors is not implied and should not be assumed.

DISCLAIMER

This research was funded through the Wisconsin Highway Research Program by the Wisconsin Department of Transportation and the Federal Highway Administration under Project # 0092-03-12. The contents of this report reflect the views of the authors who are responsible for the facts and accuracy of the data resented herein. The contents do no necessarily reflect the official views of the Wisconsin Department of Transportation or the Federal Highway Administration at the time of publication.

This document is disseminated under the sponsorship of the Department of Transportation in the interest of information exchange. The United State Government assumes no liability for its contents or use thereof. This report does not constitute a standard, specification or regulation.

The United States Government does not endorse products or manufacturers. Trade and manufacturers' names appear in this report only because they are considered essential to the object of the document.

Technical Report Documentation Page

1. Report No. 0092-03-12	2. Government Accession No	3. Recipient's Catalog No
4. Title and Subtitle DEVELOPMENT OF METHODOLOGY TO INCLUDE THE STRENGTH CONTRIBUTION OF SELECT SUGRADE MATERIALS IN PAVEMENT STRUCTURE		5. Report Date 6. Performing Organization Code
7. Authors Tuncer B. Edil, Craig H. Benson, Woon-Hyung Kim, and Burak F. Tanyu		8. Performing Organization Report No.
9. Performing Organization Name and Address Department of Civil and Environmental Engineering University of Wisconsin-Madison 1415 Engineering Drive Madison, WI 53706		10. Work Unit No. (TRAIS) 11. Contract or Grant No.
12. Sponsoring Agency Name and Address Wisconsin Department of Transportation 4802 Sheboygan Avenue Madison, WI 73707-7965		13. Type of Report and Period Covered 14. Sponsoring Agency Code
15. Supplementary Notes		

16. Abstract

This study was conducted to develop a methodology to incorporate the structural contribution of working platforms, including those constructed with industrial by-products, into the design of flexible pavements. Structural contribution of the working platform was quantified in terms of a structural number or an effective roadbed modulus. Resilient modulus obtained from large-scale model experiments (LSME) conducted on several working platform materials (i.e., crushed stone (referred to as "breaker run", Grade 2 granular backfill (referred to as Grade 2), foundry slag, foundry sand, and bottom ash) were used in the analysis. Design charts are presented that show the structural number or the roadbed modulus as a function of type of material and thickness of the working platform.

Another study was conducted to evaluate the structural contribution of geosynthetic-reinforced granular layers that are used as working platforms to the pavement structure. Based on the LSME and from the field Falling Weight Deflectometer (FWD) tests, the relationship between back-calculated elastic modulus and bulk stress was obtained. The improvement in layer coefficients is rather small for the nonwoven geotextile and drainage geocomposite (10%) and somewhat higher for the geogrid (40%) and for the woven geotextile (18%) in a 0.30-m thick granular working platform layer (treated as a subbase). The contribution of geosynthetics would be even less having a thicker subbase layer.

17. Key Words working platform, industrial by-product, geosynthetic, structural contribution, modulus, subgrade reinforcement, crushed rock, gravel, equivalency, beneficial reuse	18. Distribution Statement No restriction. This document is available to the public through the National Technical Information Service 5285 Port Royal Road Springfield VA 22161

19. Security Classif.(of this report) Unclassified	19. Security Classif. (of this page) Unclassified	20. No. of Pages	21. Price

Form DOT F 1700.7 (8-72) Reproduction of completed page authorized

EXECUTIVE SUMMARY

The objective of this study was to develop a methodology for incorporating the structural contribution of a working platform into the AASHTO design method for pavements. Two approaches have been proposed for flexible pavements. In one approach, the structural contribution of the working platform is included by defining a structural number for the working platform as if it was a subbase. In the other approach, the contribution of the working platform is included using a composite effective roadbed modulus. The structural number approach is more direct and is preferred. However, in some cases the structural number approach indicates that the working platform provides no structural contribution, whereas some improvement to the pavement system is expected when a strong working platform is placed on top of a soft subgrade. In such cases, the composite effective roadbed modulus is used.

Two design charts were presented that relate the structural number or the combined effective roadbed modulus to the thickness of the working platform. The 'structural number chart' provides the layer structural number for various working platforms as a function of thickness. If this chart indicates that the working platform provides no additional pavement support (i.e., the chart yields a structural number = 0), then the combined effective roadbed modulus chart is used. The modulus from the combined effective roadbed modulus chart is then used in the AASHTO nomograph equation when determining the required SN of the pavement. A composite modulus of subgrade reaction was determined from the combined effective roadway modulus for use in design of rigid pavements for various working platforms as a function of thickness. These tables and charts are based on the mechanical properties of the working platform materials that were used in this study and apply to cases where the subgrade is very soft (CBR of 1-3). For stronger subgrades, it is expected to provide a somewhat conservative recommendations. Therefore, the use of the charts are limited to the materials considered in this study and should be considered as examples of how the structural contribution of working platforms can be incorporated into pavement design.

Another study was conducted to evaluate the structural contribution of geosynthetic-reinforced granular layers that are used as working platforms during construction over soft subgrade, to the pavement structure under in-service loads. Four geosynthetics (geogrid, woven geotextile, nonwoven geotextile, and drainage geocomposite) were considered. Moduli of the reinforced working platforms were obtained from prototype-scale tests conducted in the laboratory on simulated pavement systems and field tests on test sections incorporated into a secondary highway in Wisconsin. The effect of geosynthetics was expressed in terms of the "reinforcement factor," which is defined as the elastic modulus of the geosynthetic-reinforced working platform divided by the elastic modulus of an unreinforced working platform having the same thickness and constructed with the same granular material.

Working platforms reinforced with geosynthetics had smaller elastic deflections and larger elastic moduli than unreinforced working platforms having the same thickness. Reinforcement factors ranging from 1.2 to 1.8 were obtained in the field and 1.7 to 2.0 in the laboratory, with greater reinforcement factors for the less extensible geosynthetics (geogrid, woven geotextile) for a 0.3 m-thick granular working platform. Of the four geosynthetics tested, the geogrid resulted in the greatest increase in modulus.

Structural contributions of the working platforms were estimated by treating them as a subbase in the conventional AASHTO design method for pavements. Reinforcing the working platforms with geosynthetics resulted in increases in layer coefficients ranging from 50 to 70%. Similarly, increases in structural number for a typical flexible pavement structure were realized ranging from 3 to 11%, with the largest increase for the geogrid. Composite modulus of subgrade reaction needed in the design of rigid pavements can be estimated from the resilient moduli of geosynthetic-reinforced layer and an assumed soft subgrade modulus..

TABLE OF CONTENTS

LIST OF TABLES

LIST OF FIGURES

CHAPTER ONE

DEVELOPMENT OF METHODOLOGY TO INCLUDE STRUCTURAL CONTRIBUTION OF ALTERNATIVE WORKING PLATFORMS IN PAVEMENT STRUCTURE

1.1 INTRODUCTION

Building a working platform during construction to support equipment is a common practice in many states such as Wisconsin when poor subgrade conditions are encountered (WisDOT 1997). The thickness and material of the working platform are typically chosen to limit total deflection of the working platform under the construction traffic (Crovetti and Schabelski 2001). Despite its importance during construction, working platform is not necessarily considered as part of the pavement system in supporting the post-construction vehicular traffic.

Design of pavement structures may show variations from one agency to another or from one state to another but the most current and most commonly used design guideline in the United States is the *AASHTO Guide for Design of Pavement Structures*, which is prepared by the American Association of State Highway and Transportation Officials (AASHTO) in 1993 (Newcomb and Birgisson 1999). The AASHTO (1993) flexible pavement design guide does not consider specifically the structural contribution of working platform. The pavement structure is designed based on the properties of subgrade.

When the subgrade consists of soft soil, the pavement structure is either designed by using a thicker base course and/or asphalt layer or by building an extra

support layer (i.e., subbase). Either approach results in increased overall cost. However, significant savings could be realized if the working platform, which is already constructed to implement construction over poor soils could be incorporated into pavement design.

This study was performed to develop a methodology to incorporate the structural contribution of the working platform into pavement design for performance under in-service loads after construction. Another project addresses the design of working platforms for performance during construction (WHRP Project SPR #92-00-12).

1.2 BACKGROUND

Understanding the existing design procedure is necessary in order to evaluate the structural contribution of the working platform. This study uses the design procedure developed by the AASHTO in 1993 since this design guideline is the latest national design guideline available and also followed by many agencies in the United States (Newcomb and Birgisson 1999). The design procedure for both pavements is based largely on the results of the AASHO Road Test in Ottawa, Illinois conducted in the late 1950s and early 1960s (AASHTO 1993). Empirical equations based on field observations from the AASHTO Road Test are employed to relate the design period, traffic, reliability, environmental effects, serviceability, and subgrade condition to determine the design structural number required from a pavement structure.

Two elements of the AASHTO design procedure are particularly important in determining the structural contribution of the working platform: (i) the structural number and (ii) effective roadbed resilient modulus. The structural number is a function of layer coefficients and layer thicknesses of all pavement layers (AASHTO 1986) where the layer coefficient is a function of the resilient modulus of the layer (Rada and Witczak 1981). Effective roadbed resilient modulus is an estimated roadbed modulus value that includes the seasonal moisture condition effects to the modulus and incorporates the relative damage that would be caused due to the modulus of the roadbed (AASHTO 1993, Elliot and Thornton 1988).

For a given set of design inputs, a nomograph in the AASHTO (1993) design guide is used to obtain the design structural number (SN). The equation that the AASHTO (1993) nomograph is based on is given below:

$$\log_{10} W_{18} = z_R S_o + 9.36\log_{10}(SN+1) - 0.20 + \frac{\log_{10}\left[\frac{\Delta PSI}{4.2 - 1.5}\right]}{0.40 + \frac{1094}{(SN+1)^{5.19}}} + 2.32\log_{10} M_r - 8.07 \quad (1.1)$$

where W_{18} is the estimated total equivalent single axle load, Z_R is the reliability factor that is a function of the overall standard deviation, S_o, which accounts for both the variation in traffic prediction and variation in pavement performance prediction for a given W_{18}, ΔPSI is the design service ability loss, and M_r is the effective roadbed resilient modulus.

SN in Eq. 1.1 is a design number representing the required structural capacity of the pavement structure and depends on the mechanical properties of the materials constituting the pavement layers and their thicknesses. The design SN is the summation of the structural number of each pavement layers as shown in Eq. 1.2 below:

$$SN = SN_1 + SN_2 m_2 + SN_3 m_3 \quad (1.2)$$

where SN_i is the structural number of the layer i and m_i is the drainage modification factor for layer i. Properties of each pavement layers are described within the structural number by their layer coefficients. The relationship between design structural number and layer coefficients are defined as given in Eq. 1.3.

$$SN = a_1 D_1 + a_2 D_2 m_2 + a_3 D_3 m_3 \quad (1.3)$$

where a_i is the layer coefficient of the layer i and D_i is the thickness of the layer i in English units of inches.

The layer coefficient is a measure of the effectiveness of a given material to function as a structural component of the pavement. The layer coefficient has been related to the resilient modulus (M_r) of the layer material in the 1993 AASHTO

guideline using the empirical equations developed by Rada and Witczak (1981). For example, for granular subbase material the relationship is given in Eq. 1.4.

$$a_3 = 0.227 \log (M_r)_3 - 0.839 \quad (1.4)$$

where a_3 is the layer coefficient and $(M_r)_3$ is the resilient modulus of the granular subbase material in English units of pounds per square inch.

Since the completion of this project, Transportation Research Board published Guide for Mechanistic-Empirical Pavement Design, (NCHRP 2004) which essentially requires a modulus and a Poisson's ratio (often estimated) for each pavement layer. Therefore, the moduli reported in this report would be applicable for use in the new design guidelines.

A literature survey showed that there is limited published literature regarding resilient modulus and plastic strain accumulation of industrial by-products; however, the mechanical behavior of granular natural materials are widely studied and the results are summarized in literature (Arellano and Thompson, 1999; Huang 1993, Witczak 2003).

1.3 MATERIALS

The Wisconsin Department of Transportation has identified eight select material alternatives for stabilization of soft subgrades. This list of select materials is composed of:

1. Breaker run stone
2. Breaker run stone with geogrid
3. Grade 1 granular backfill
4. Grade 2 granular backfill
5. Pit run sand and gravel
6. Pit run sand and gravel with geogrid
7. Flyash, lime and cement stabilization
8. Salvage materials or industrial by-products with optional geogrid

In developing the testing philosophy, an approach that would yield general relationships that can be adapted to specific materials based on laboratory material property characterization was adopted rather than testing these 8 alternative materials. Furthermore, use of field data to validate the approach is critical. Thus, the available field test sections and materials constrained the choices. Therefore, a generalized approach was developed using the large-scale laboratory experiments with the results validated in the field. This approach can be applied to other granular materials, chemical stabilization methods, or geosynthetics using the procedures described in this report. Thus, although tests were not conducted on each of the materials listed above, the method we developed can be used to design with any of the materials.

The properties of the working platform materials considered are summarized in Table 1.1. All of the materials are coarse-grained and granular. They classify as crushed rock (referred to as “breaker run”), gravel (Grade 2 granular backfill which

is referred to as “Grade 2”), and sand (industrial by-products: bottom ash, foundry slag, and foundry sand). Breaker run is a natural material and commonly used as a working platform material in many states. Grade 2 is crushed or natural aggregate that is screened to meet the Gradation No. 2 requirements for granular backfill stated in WisDOT’s *Standard Specifications for Highway and Structure Construction* (WisDOT 1996). Bottom ash, foundry slag, and foundry sand are industrial by-products that can be used as alternative working platform materials over soft subgrades. Breaker run and Grade 2 were produced from dolostone rock. Foundry slag is referred to as tap slag, which is produced as a result of cupola water quenching by the gray iron casting industry. Bottom ash is a by-product of coal combustion in electrical power plants. Foundry sand, which is a by-product of the gray iron casting industry, included 10% bentonite as the binder and seacoal (powdered coal) as the combustible additive. All of the materials used except the foundry sand are nearly insensitive to water content changes during compaction. Foundry sand was specified to be tested at optimum water content (i.e., 16%) (Edil et al. 2002).

Table 1.1. Properties of working platform materials.

Material	Specific Gravity	D_{10} (mm)	D_{60} (mm)	C_u	% Fines	USCS Symbol	AASHTO Symbol	Max. Dry Unit Weight (kN/m^3)		Optimum Water Content per ASTM D 698 (%)	CBR
								Compaction per ASTM D 698	Vibratory per ASTM D 4253		
Breaker Run	NM[a]	0.25	29	116	3.1	-	-	NM[a]	NM[a]	--	80
Grade 2	2.65	0.090	6.0	67	7.9	GW	A-1-a	22.6	NM[a]	--	33
Bottom Ash	2.65	0.060	1.9	32	13.2	SW	A-1-b	15.1	13.7	--	21
Foundry Slag	2.29	0.13	2.0	15	5.3	SW	A-3	10.0	8.4	--	12
Foundry Sand	2.55	0.0002	0.23	1150	28.9	SC	A-2-7	16.1	NM[a]	16	2 – 25[b]

Notes: [a]NM = not measured, [b]un-soaked CBR varies with compaction water content.

1.4 RESILIENT MODULUS OF THE WORKING PLATFORM MATERIALS

The resilient modulus of the materials were determined by Tanyu et al. (2003) from an analysis of the large-scale model experiments (LSME) using KENLAYER, a computer program developed by Huang (2004) for analysis of pavement structures as a layered system of linear or non-linear elastic materials. The LSME is an experimental setup devised to model a pavement structure (or parts of it) at the prototype scale in a manner that replicates field conditions as closely as practical. Therefore, large-scale model experiments incorporate not only the effect of stress on modulus but also the effect of strain amplitude on modulus. Furthermore, the moduli provided by the LSME are shown to be relevant to the operative modulus in a working platform in the field based on an analysis of field falling weight deflectometer data (2003). The use of the resilient modulus based on the (AASHTO T 294), while incorporating the stress effects on modulus, would not have taken the strain amplitude effect into account. The conventional specimen resilient modulus test would give lower operating moduli than what is observed in the field and the LSME. Details of the LSME can be found in Tanyu et al. (2003). The schematic cross section of LSME is shown in Fig. 1.1 and a brief explanation is given below.

The material layers in the LSME included from bottom up a layer of dense uniform sand, a simulated soft subgrade, and the working platform test material. The

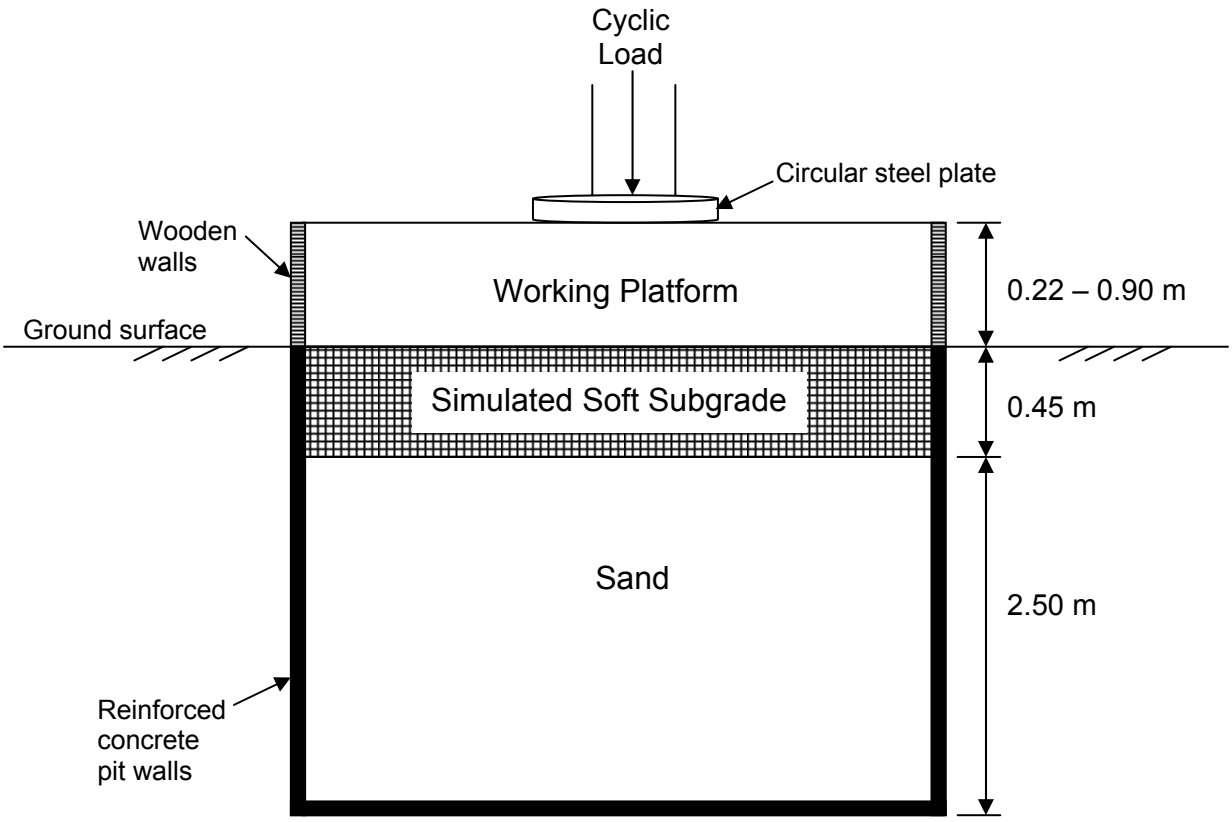

Fig. 1.1. Schematic cross section of Large-Scale Model Experiment (LSME).

sand had an effective grain size of 0.22 mm, a coefficient of uniformity of 1.8, a dry unit weight of 17.4 kN/m^3, a void ratio of 0.49 and had a relative density of 85%. The simulated soft subgrade consisted of expanded polystrene (EPS) blocks that replicate the deformational response of a soft subgrade in the range of stresses applied in the LSME. The soft subgrade simulated corresponds to a least suitable subgrade soils in Wisconsin with a CBR of $\leq$ 1 and a M_r of 1 MPa. The working platform materials were placed in 0.11-m-thick lifts and each lift was compacted to a dry unit weight in excess of 95% of the maximum standard Proctor dry unit weight.

Testing materials were subjected to two stages of repetitive loading: (i) higher intensity loading with small number of cycles (i.e., 1,000) simulating heavy truck traffic directly over the working platform during construction and (ii) lower intensity loading with large number of cycles (i.e., 10,000) simulating vehicular traffic on the finished pavement.

The second stage of loading (i.e., the lower intensity loading that is of primary concern for this phase of the study) was selected to simulate the stress induced at the working platform level by the surface vehicular traffic load. The induced load was calculated to be approximately 20% of the applied load on the surface of the pavement for a typical pavement structure (i.e., 140 kPa stress due to a 7 kN wheel load) (2003). Load was applied using a haversine load pulse consisting of a 0.1-s load period followed by a 0.9-s rest period, the same load pulse specified in the small-scale laboratory resilient modulus test.

Resilient modulus of the working platform materials were obtained by inversion from KENLAYER using the data obtained from the LSME. In the inversion analysis, moduli of the working platform layers was assumed to follow the non-linear elastic k-σ_b model:

$$M_r = k_1 \sigma_b^{k_2} \quad (1.5)$$

where k_1 and k_2 are empirical constants and σ_b is the bulk stress. This model has been shown to be a satisfactory model for a wide range of granular materials (Hicks and Monismith 1971).

An example of the back-calculated resilient modulus as described in Tanyu et al. (2003) is shown in Fig 1.2. k_1 and k_2 are the empirical constants of the model and they are listed in Table 1.2 for all of the working platform materials considered in this study.

1.5 DETERMINATION OF WORKING PLATFORM CONTRIBUTION USING STRUCTURAL NUMBER FOR FLEXIBLE PAVEMENTS

The most direct approach to determine the structural contribution of a working platform in the context of the 1993 AASHTO guide is to treat the working platform as a subbase and determine a layer coefficient for the subbase using Eq. 1.4, which in

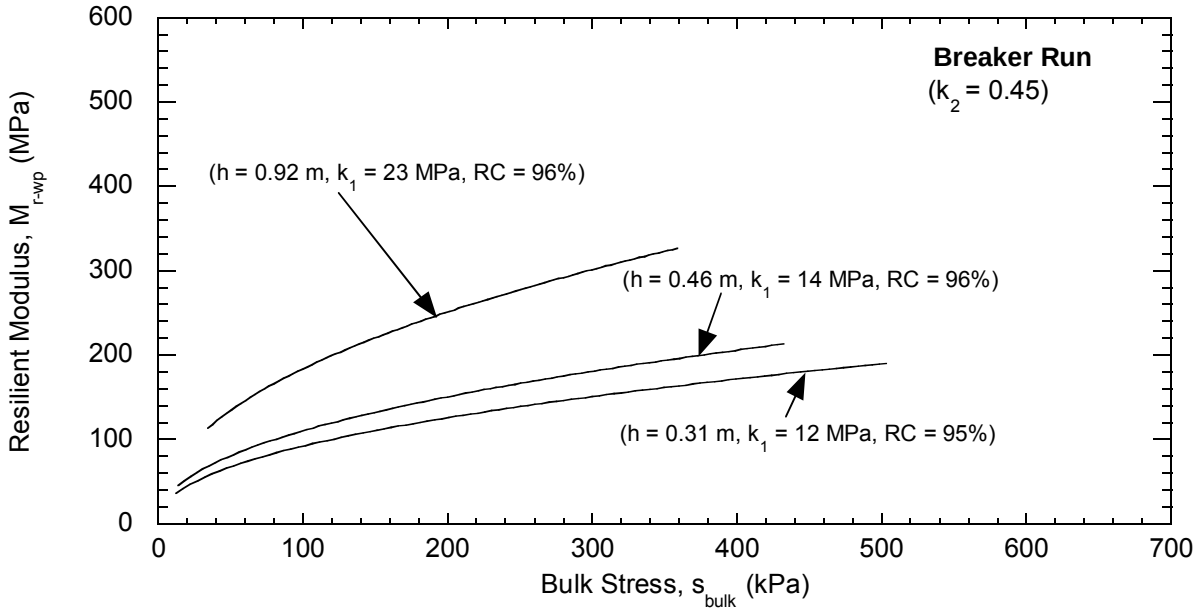

Figure 1.2. The inverted resilient modulus of the breaker run.

Table 1.2. Empirical constants of resilient modulus of subbase layers.

Material		Thickness of the Working Platform, h (m)	Empirical Constants[a]	
			k_1 (Mpa)	k_2
Breaker run		0.31	12	0.45
		0.46	14	
		0.91	23	
Grade 2		0.31	6	0.50
		0.46	14	
Bottom ash		0.46	5	0.52
		0.69	10	
		0.91	12	
Foundry Slag		0.46	2	0.62
		0.91	3	
Foundry Sand	w = 16%	0.46	106	0.23
		0.69	119	
		0.91	133	

Note: [a] $M_r = k_1 \sigma_b^{k_2}$, where M_r is the resilient modulus and σ_b is the bulk stress.

turn can be implemented in Eq. 1.3. For this purpose, a chart showing the relationship between the structural number of a working platform layer (SN_3) and the thickness of the working platform (h) is developed, thus a SN_3 can be assigned to a working platform based on its thickness, which is usually defined during the construction phase. SN_3 is a function of the layer coefficient (a_3) and the working platform thickness (h) (Eq. 1.3), and the layer coefficient is a function of resilient modulus of the working platform ($M_{r\text{-}wp}$) (Eq. 1.4).

As can be seen from Fig. 2, the resilient modulus of a working platform is not constant but depends on the bulk stress but also on the thickness of the working platform as explained in Tanyu et al. (2003). This is due to the non-linear dependence of resilient modulus on bulk stress as well as on strain-amplitude. Working platform thickness controls the level of induced strains for a given load. Therefore, a representative bulk stress, such as at mid-depth of the working platform, is needed to determine an operating resilient modulus for the layer.

1.5.1 Determining Representative Bulk Stress in Working Platform

The bulk stress is the summation of all principal stresses both due to geostatic stresses and induced stresses by surface loads (Huang 2004). For a given pavement structure, the bulk stress in the mid-depth of a working platform for a given surface load depends on the moduli, unit weight, and thickness of the overlying layers as well as the thickness of the working platform itself. Literature suggests that typical asphalt and base layer thicknesses do not vary much (Huang

2004, Barksdale 1971, Tutumluer and Thompson 1997, Thompson 1999, Hayden et al. 1999, Nazarian et al. 2003, WisDOT 2003). For instance, typical thickness of asphalt concrete (AC) layer ranges between 0.10 and 0.25 m and typical thickness of base layer ranges between 0.15 and 0.41 m. As a common practice a thin AC layer usually is associated with a thicker base layer and a thicker AC is associated with a thinner base layer.

Bulk stress in the mid-depth of the working platforms considered here were determined using the KENLAYER program. Two pavement profiles were simulated for the overlying layers above the working platform to bracket the operating bulk stress range. Profile 1 was a thin AC layer (0.10 m) combined with a thick base layer (0.41 m) and Profile 2 was a thick AC layer (0.25 m) combined with a thin base layer (0.15 m). The properties of the working platform materials needed in the analysis are given in Table 1.2. The moduli and unit weights of the asphalt and base layers were assumed. The asphalt was assumed to have a resilient modulus of 2,480 MPa, which corresponds to the moduli of asphalt at typical summer temperature, i.e., 25^{o}C (Michala and Scullion 1987) and a Poisson's ratio of 0.30 (Huang 2004). The base course was assumed to have a resilient modulus of 175 MPa, unit weight of 21.2 kN/m^3, and a Poisson ratio of 0.35 (corresponding to a at-rest earth pressure coefficient of 0.54). The applied load that was simulated in the KENLAYER program was selected to be 700 kPa corresponding to typical tire pressure of a truck.

The sensitivity of the bulk stress analysis to the assumed properties of asphalt and base course was evaluated for practical ranges. The asphalt modulus is a function of temperature and two extreme asphalt moduli were selected for the bulk stress evaluation. At 4^{o}C the asphalt modulus is 14,000 MPa and at 43^{o}C the asphalt modulus is 1,300 MPa (Michala and Scullion 1987). Assuming everything being the same, the difference between the bulk stresses calculated in the middle of the working platform for the 14,000 MPa and 1,300 MPa asphalt moduli was 0.25 kPa, which shows that the bulk stress in the middle of the working platform is not sensitive to the assumed asphalt moduli for the typical range of values.

The practical range for granular base moduli is between 137 MPa and 206 MPa (Huang 2004, Yoder and Witczak 1975). Assuming everything being the same the difference between the bulk stresses calculated in the middle of the working platform for 137 MPa and 206 MPa base moduli was 0.70 kPa, which shows that the bulk stress in the middle of the working platform is also not highly sensitive to the assumed base moduli for the typical ranges of values as well.

Fig. 1.3 provides an example of the bulk stresses calculated in the mid-depth of a working platform constructed with breaker run for the two AC/base layer profiles described above. Two observations can be made. First, for a given working platform thickness, bulk stress calculated in the mid-depth of the working platform is approximately the same within 1 kPa for either profile of the AC and base layer. Second, bulk stress increases approximately linearly with increasing working

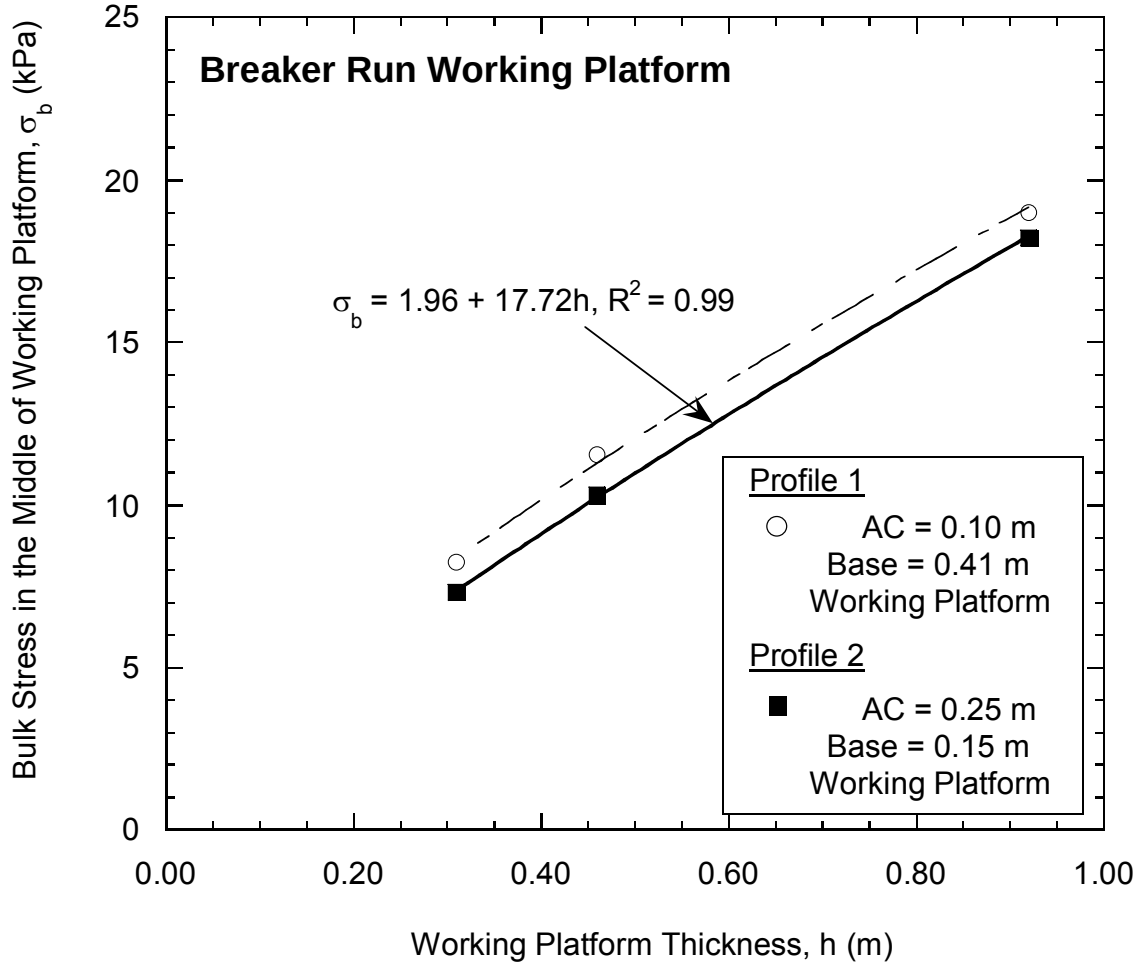

Figure 1.3. Bulk stresses calculated in the middle of the breaker run working platforms with two different pavement structure profiles.

platform thickness implying that bulk stress is controlled primarily by the increase in geostatic stresses.

In order to generalize the bulk stress-working platform thickness relationship, the following linear function was fitted to the data from all working platform materials for the assumption of Profile 2 for the overlying layers:

$$\sigma_b = \chi + \eta h \qquad (1.6)$$

where χ and η are the fitting parameters for σ_b in kPa and h in m. The parameters χ and η for all materials are summarized in Table 1.3. The R^2 associated with these fits range between 0.97 and 1.00 indicating a strong correlation. Profile 2 was used in calculations because bulk stresses calculated based on profile 2 were slightly smaller and therefore corresponded to more conservative resilient modulus values. At any rate, the effect of the overlying layers within their thickness and moduli ranges on bulk stress in the middle of the working platform is not significant.

1.5.2 Determining Operating Modulus and Layer Coefficient of Working Platform

Bulk stresses corresponding to various working platform thicknesses were calculated using Eq. 1.6 and the corresponding parameters from Table 1.3 for each material. Some of the bulk stress values were extrapolated using Eq. 1.6. Using the calculated mid-depth bulk stresses, the operating working platform modulus ($M_{r\text{-}wp}$)

Table 1.3. Linear fit parameters to σ_b – h relationship of working platform materials.

Material		Eq. 6 Parameters		
		χ	η	R^2
Breaker run		1.96	17.72	0.99
Grade 2		-1.31	21.33	1.00
Bottom ash		0.08	11.67	0.98
Foundry Slag		0.96	6.84	1.00
Foundry Sand	[a]w = 16%	5.38	12.22	0.97

Note: [a]w = water content.

at a given thickness was estimated from the resilient modulus versus bulk stress plots like in Fig. 1.2 that were obtained for each material in the LSME. As explained previously, the moduli estimated on the basis of conventional specimen resilient modulus tests were not used. The corresponding working platform a_3 was calculated from the operating $M_{r\text{-}wp}$ using Eq. 1.4 with the assumption that this equation is also applicable for other granular materials such as industrial by-products used in this study. From the a_3 data covering a range of thicknesses, SN_3 was calculated using Eq. 1.3 and the results are plotted in Fig. 1.4. SN_3 is noted to depend on working platform thickness both directly as in Eq. 1.3 and also through the dependence of a_3 on thickness.

Foundry slag was not included in this figure because Eq. 1.4 yielded negative a_3 values for foundry slag within all reasonable range of working platform thicknesses (i.e., up to 1.5 m) for that material. Although foundry slag does not appear to qualify as a subbase layer, there is no question that foundry slag does reinforce the soft subgrade. The second approach using a composite effective roadbed resilient modulus, as explained later, was adopted for incorporating the contribution of foundry slag.

1.5.3 Practical Implication of Structural Number-Layer Thickness Chart

For any given working platform thickness, the designer can determine whether the working platform can be incorporated into pavement design as a subbase layer or not. For example, if the working platform is built with bottom ash

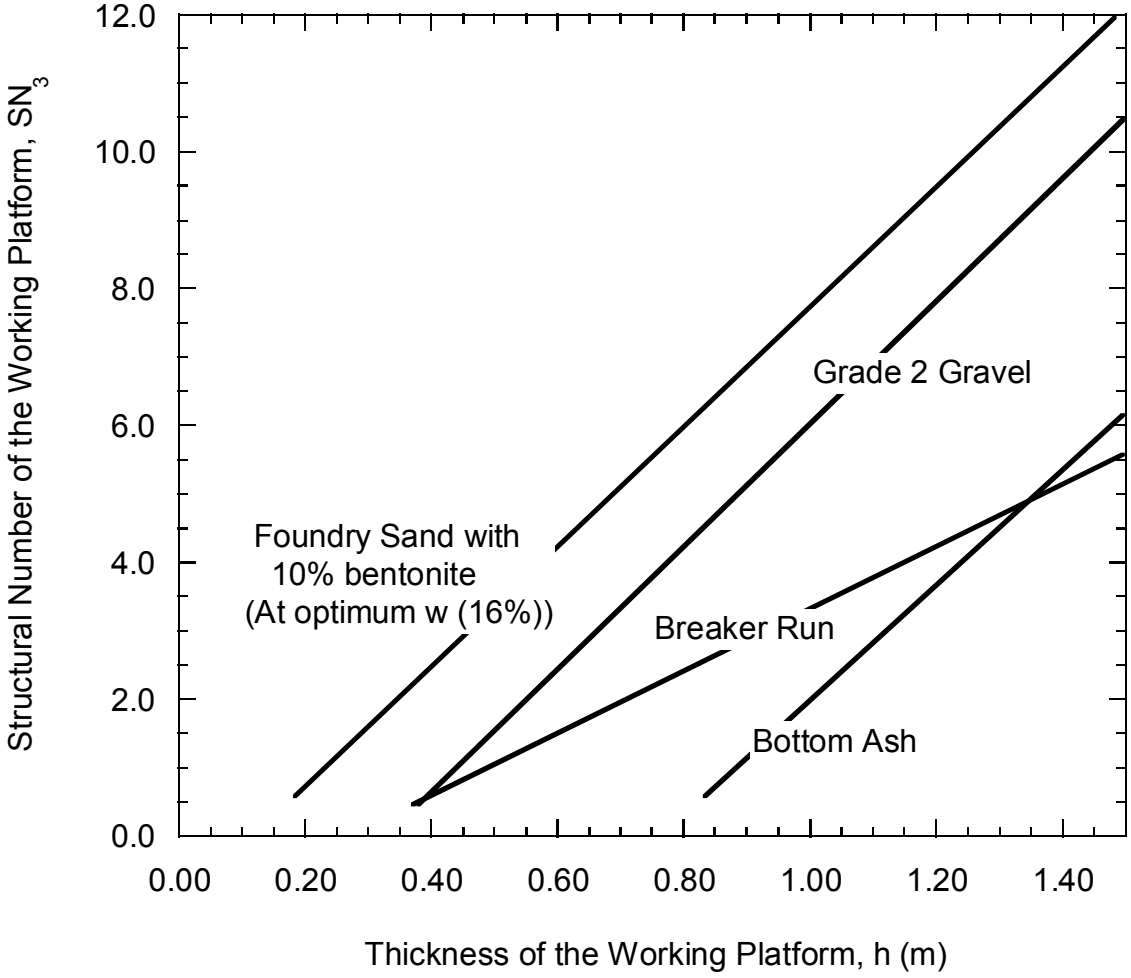

Figure 1.4. Relationship between structural number of the working platform and the thickness of the working platform.

and has a thickness of 1m, bottom ash can be included in the pavement design as a subbase because the 1-m thick bottom ash has SN_3 = 2.0, a number that is greater than 0. If the same working platform is built as 0.8 m or less, the working platform cannot be incorporated into pavement design as a subbase layer because in this case $SN_3 \leq 0$. In reality there would be some benefit but the benefit of this thin layer may be minor enough that it should not be considered for pavement design purposes.

The structural number-layer thickness chart can also be used in conjunction with the working platform design chart (i.e., thickness of alternative materials to breaker run required to limit the total deflection during construction to 12.5, 25, 37.5, and 50 mm) developed by Tanyu et al. (2004). The designer can determine the thickness of the working platform based on the construction phase considerations and determine whether or not the resulting working platform can be incorporated into pavement design as a subbase using Fig. 1.4. Examples are summarized in Table 1.4.

As can be seen from Table 1.4 the thicknesses of the working platforms to limit the total deflection during construction do not always produce a structural number for the pavement structure. This is because the $M_{r\text{-}wp}$ corresponding to the required working platform thickness is either not enough to produce a positive SN_3 or the required thickness becomes too large to be considered cost-effective. The working platform thicknesses that are considered economical are limited to 1.5 m in this study based on general practice (WisDOT 1997).

Table 1.4. Structural contribution of the working platforms in terms of structural number for working platform thicknesses required to satisfy the total deflection criteria during construction (Tanyu et al. 2004).

Materials	δ_t = 12.5 mm (0.5 in)		δ_t = 25.0 mm (1.0 in)		δ_t = 37.5 mm (1.5 in)		δ_t = 50.0 mm (2.0 in)	
	h, m (in)	SN_3	h, m (in)	SN_3	h, m (in)	SN_3	h, m (in)	SN_3
Breaker run	0.86 (34)	0.07	0.41 (16)	0.01	0.27 (11)	N.A.	0.20 (8)	N.A.
Grade 2	0.91 (36)	0.14	0.42 (17)	N.A.	0.31 (12)	N.A.	0.25 (10)	N.A.
Bottom ash	1.29 (51)	0.11	0.98 (39)	0.04	0.84 (33)	0.01	0.75 (30)	N.A.
Foundry Slag	4.60 (181)	N.E.	2.55 (100)	N.E.	1.80 (71)	N.E.	1.41 (56)	N.A.
Foundry Sand Optimum w (i.e., 16%)	0.66 (26)	0.12	0.32 (13)	0.05	0.21 (8)	0.03	0.15 (6)	0.02

Notes: N.E.: Not economical to built due to the thickness required, N.A.: Structural number is ≤ 0, h: Working platform thickness,. δ_t: Total deflection of working platform due to construction phase loading

Placing a working platform on soft subgrade reinforces the soft subgrade regardless of whether working platform can be treated as a subbase layer with a structural number. The next section explains how the structural contribution of a working platform can be incorporated into pavement design in terms of a composite roadbed resilient modulus.

1.5.4 Determining Working Platform Contribution in Terms of Composite Roadbed Resilient Modulus

Soft subgrade and the working platform built on top of soft subgrade form a two-layer roadbed system underneath the pavement structure with some beneficial effect even if the working platform is not to the level of a subbase layer. In a two-layer elastic system the load distributed to the bottom layer would depend on the ratio of the elastic modulus of the upper layer (i.e., working platform ($M_{r\text{-}wp}$), the elastic modulus of the bottom layer (i.e., subgrade ($M_{r\text{-}sub}$)), the thickness of the upper layer, and the size of the loading area (Burmister 1958). Knowing the working platform thickness (h), $M_{r\text{-}wp}$, and $M_{r\text{-}sub}$, a composite resilient modulus that represents the roadbed ($M_{r\text{-}comp}$) can be determined from the analytical solution of a two-layer elastic system developed by Ueshita and Meyerhof (1967). The soft subgrade is assumed to be of large depth in this solution. Because of a low modulus assumption for the soft subgrade, i.e., 1 MPa, the composite roadbed modulus can be used as a conservative effective roadbed resilient modulus for a range of poor subgrades following the AASHTO (1993) pavement design guide.

A chart showing the relationship between composite roadbed resilient modulus ($M_{r\text{-}comp}$) and working platform thickness (h) is developed based on the Ueshita and Meyerhof (1967) solution and presented in Fig. 1.5 (Note that $M_{r\text{-}sub}$ = 1 MPa). For $M_{r\text{-}wp}$, the modulus corresponding to various working platform thicknesses were obtained using first the σ_b – h relationship given in Eq. 1.6 and then the $M_{r\text{-}wp}$ – σ_b relationship given in Eq. 1.5.

The $M_{r\text{-}comp}$ – h chart (Fig. 1.5) has practical implications when used in conjunction with SN_3 – h (Fig. 1.4) chart. Working platform thicknesses that do not result in $SN_3 > 0$, can still be incorporated into pavement design through the composite roadbed resilient modulus using Fig. 1.5. For example, based on Table 1.4 a working platform built with Grade 2 that has a thickness of 0.42 m does not produce a $SN_3 > 0$; however, 0.42-m-thick Grade 2 can still be incorporated into the pavement design with a composite roadbed resilient modulus of 8 MPa as opposed to 1MPa of the subgrade that would be used.

Incorporating working platform into pavement design with a composite roadbed resilient modulus does not necessarily eliminate the need of designing a subbase layer for economic reasons.

1.6 DETERMINATION OF WORKING PLATFORM CONTRIBUTION USING COMPOSITE MODULUS OF SUBGRADE REACTION FOR RIGID PAVEMENTS

If the working platform is treated like a subbase between the concrete pavement slab and the subgrade, the composite modulus of subgrade

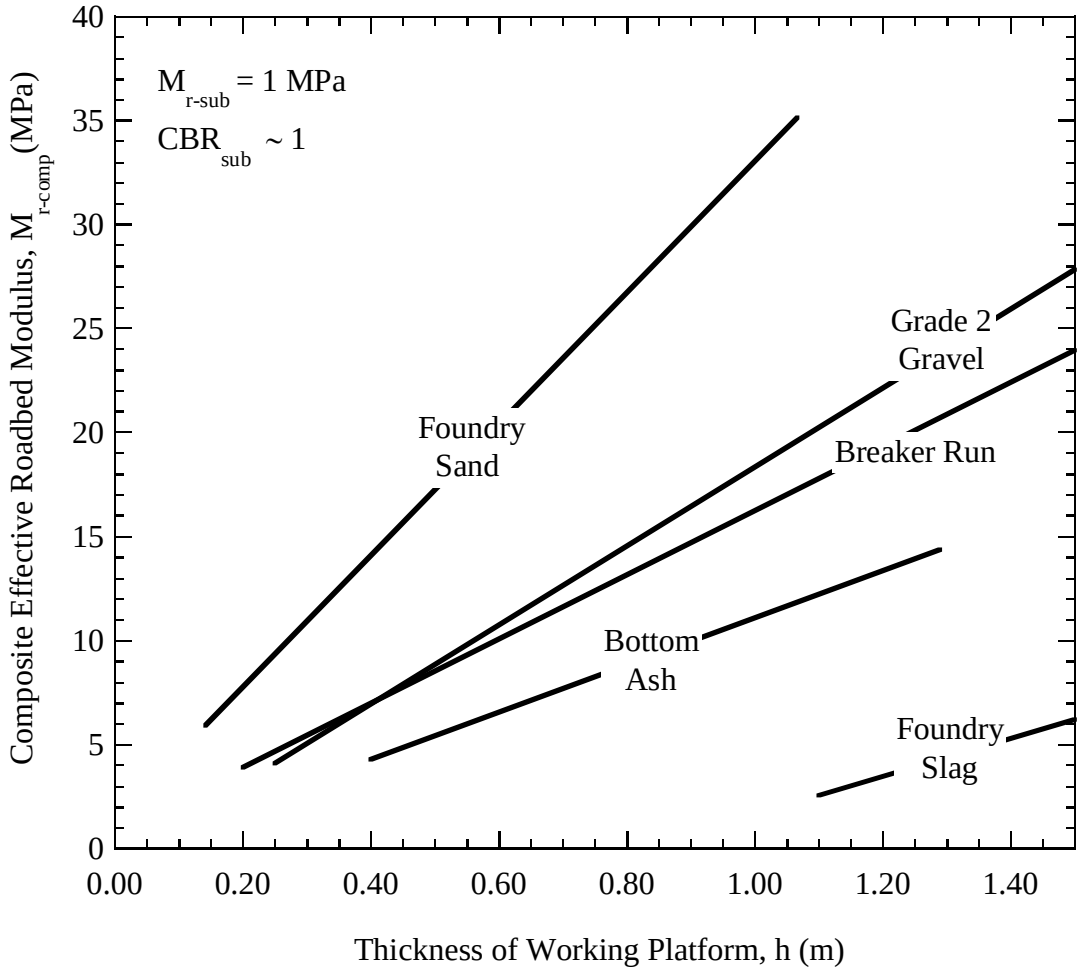

Figure 1.5. Relationship between roadbed resilient modulus and the thickness of the working platform.

reaction, k_∞ (in MN/m^3) can be determined from the composite roadbed resilient modulus as described in Section 1.5.4 based on the same assumptions made earlier using (Huang 2004)

$$k_\infty = \frac{2M_{r\text{-}comp}}{\pi(1-\upsilon^2)a} = \frac{M_{r\text{-}comp}}{2.1} \quad (1.7)$$

where $M_{r\text{-}comp}$ (in MPa) is as defined in Section 1.5.4, υ is the Poisson's ratio of the foundation (assumed to be 0.45), and a is the radius of the loading plate or area (assumed to be 0.381 m). Table 1.5 provides the composite modulus of subgrade reaction for various types of working platforms.

1.7 SUMMARY AND CONCLUSIONS

The primary goal of this study was to develop a methodology where the structural contribution of a working platform to pavement structures could be incorporated into pavement design. Two approaches were used to incorporate the structural contribution of a working platform on the basis of the AASHTO (1993) design guide for pavements for flexible pavements. In the first approach, the structural contribution of the working platform is included in pavement design in a manner similar to that of a subbase, which meant determining a structural number for the working platform.

In the second approach, where the structural number of the working platform does not qualify to treat the working platform as a subbase, the working platform

Table 1.5 Composite Modulus of Subgrade Reaction for working platforms for working platform thicknesses required to satisfy total deflection criteria during construction described in (Tanyu et al. 2004).

Materials	δ_t = 12.5 mm (0.5 in)		δ_t = 25.0 mm (1.0 in)		δ_t = 37.5 mm (1.5 in)		δ_t = 50.0 mm (2.0 in)	
	h (m)	k (MN/m^3)	h (m)	k (MN/m^3)	h (m)	k (MN/m^3)	h (m)	k (MN/m^3)
Breaker run	0.86	29.4	0.41	14.7	0.27	10.5	0.20	8.4
Grade 2	0.91	37.7	0.42	16.8	0.31	10.5	0.25	6.3
Bottom ash	1.29	29.4	0.98	23.1	0.84	21.0	0.75	16.8
Foundry Slag	4.60	NE	2.55	NE	1.80	NE	1.41	11.2
Foundry Sand	0.66	46.1	0.32	25.2	0.21	16.8	0.15	12.6

Notes: NE = not economical due to excessive thickness, h = working platform thickness, δ_t = total deflection of working platform due to construction phase loading. Foundry sand assumed to be placed at optimum water content.

was treated as part of a two-layer composite roadbed soil with the other layer being the subgrade. The contribution of the working platform is assessed as an improvement on the roadbed modulus of the subgrade. Using the elastic theory, a composite roadbed modulus is calculated taking into account the moduli of the working platform, and the subgrade, and their thicknesses.

Obtaining either the structural number or the composite effective roadbed resilient modulus requires the operating resilient modulus of a working platform of a given thickness. The resilient modulus data used in this study is provided by testing crushed rock ("breaker run"), granular backfill ("Grade 2"), foundry slag (tap slag), bottom ash, and foundry sand with an optimum water content of 16% as part of a large-scale model experiment simulating a prototype-scale pavement structure.

Two design charts were developed for flexible pavements based on either the structural number or the roadbed resilient modulus. The first chart describes the relationship between the thickness of the working platform and the corresponding structural number for each of the working platform materials considered. This chart allows a designer to determine whether or not the working platform designed or constructed for the construction phase traffic can be incorporated into pavement design with a structural number similar to a subbase layer.

The second chart describes the relationship between composite roadbed resilient modulus of the working platform-subgrade system and working platform thickness. This chart is constructed to present an alternative way to incorporate the

structural contribution of the working platform into pavement design when working platform cannot be treated as a subbase.

These two charts are based on the mechanical properties of the specific but common granular working platform materials and for a very soft subgrade with CBR of 1 or less. Therefore, the use of the charts are limited to the materials considered in this study and should be considered as examples of how the structural contribution of working platforms can be incorporated into pavement design. Future studies are recommended to study other materials of working platform that can be added to these charts.

For use in rigid pavement design, composite modulus of subgrade reaction is calculated from the composite roadbed resilient modulus described above for working platforms of various materials and thicknesses and provided in tabular form.

The new Guide for Mechanistic-Empirical Pavement Design (NCHRP 2004), requires modulus as the mechanical material property to be used directly. The moduli reported for these materials therefore can be directly used in the Mechanistic-Empirical Pavement Design. Guidelines for design and construction of the working platforms using these materials and field performance over a period of 5 tears are provided in two related reports (WHRP Project SPR #92-00-12 and WHRP Project SPR #0092-45-98).

1.8 REFERENCES

AASHTO (1986), "AASHTO Guide for The Design of Pavement Structures", *American Association of State Highway and Transportation Officials Publication*, Washington, D.C.

AASHTO (1993), "AASHTO Guide for The Design of Pavement Structures", *American Association of State Highway and Transportation Officials Publication*, Washington, D.C.

Arellano, D. and Thompson, M.R. *Stabilized Base Properties (Strength, Modulus, Fatigue) for Mechanistic-Based Airport Pavement Design*. Final Report, COE Report No. 4, Center of Excellence for Airport Pavement Research, University of Illinois at Urbana-Champaign, Prepared for the Federal Aviation Administration, Urbana, IL, February, 1998.

Barksdale, R. D. (1971), "Compressive Stress Pulse Times in Flexible Pavements for Use in Dynamic Testing", *Highway Research Record*, 345, 32-44.

Burmister, D. M. (1958), "Evaluation of Pavement Systems of the WASHO Road Test by Layered Systems Method", *Highway Research Board*, 177, 26-54.

Crovetti, J. A. and Schabelski, J.P. (2001), "Comprehensive Subgrade Deflection Acceptance Criteria", *Phase III Final Report WI/SPR 02-01,* WisDOT Highway Research Study #98-1, SPR # 0092-45-95.

Edil, T., Benson, C., Bin-Shafique, M., Tanyu, B., Kim, W., and Senol, A. (2002), Field Evaluation of Construction Alternatives for Roadway Over Soft Subgrade, *Transportation Research Record*, 1786, Transportation Research Board, National Research Council, Washington, DC, pp. 36-48.

Elliot, R. P. and Thornton, S. I. (1988), "Resilient Modulus and AASHTO Pavement Design", *Transportation Research Record,* 1196, 116-124.

Hayden, S. A., Humphrey, D. N., Christopher, B. R., Henry, K. S., and FettEn, C. (1999), "Effectiveness of Geosynthetics for Roadway Construction in Cold Regions: Results of a Multi-use Test Section", *Proceedings of the 1999 Geosynthetics Conference*, Boston, MA.

Hicks, R. G. and Monismith, C. L. (1971), "Factors Influencing the Resilient Properties of Granular Materials", *Transportation Research Record*, 345, 15-31.

Huang, Y. H. (2004), "Pavement Analysis and Design", *Prentice Hall Publication*, New Jersey, 2nd Edition, 775 p.

Michala, C. H. and Scullion, T. (1987), "Modulus 5.0 User's Manual", *Texas Department of Transportation,* Research Report 1987-1, 87 pages.

Nazarian, S., Abdallah, I., Meshkani, A., and Ke, L. (2003), "Use of Resilient Modulus Test Results in Flexible Pavement Design", *Resilient Modulus Testing for Pavement Components, ASTM STP 1437*, G. N. Durham, A. W. Mar, and W. L. De Graff, Eds., American Society for Testing and Materials, West Conshohocken, PA.

NCHRP (2004) Guide for Mechanistic-Empirical Pavement Design, TRB, Washington, DC

Newcomb, D. E. and Birgisson, B. (1999), "Measuring In Situ Mechanical Properties of Pavement Subgrade Soils", *Transportation Research Board, National Research Council,* Synthesis of Highway Practice 278, 71 pages.

Rada, G. and Witczak, M. W. (1981), "Material Layer Coefficients of Unbound Granular Materials from Resilient Modulus", *Transportation Research Record*, 852, 15-21.

Tanyu, B. F., Kim, W. H., Edil, T. B., and Benson, C. H. (2003), "Comparison of Laboratory Resilient Modulus with Back-Calculated Elastic Moduli from Large-Scale Model Experiments and FWD Tests on Granular Materials", *Resilient Modulus Testing for Pavement Components, ASTM STP 1437, Paper ID 10911*, G. N. Durham, A. W. Marr, and W. L. De Groff, Eds., ASTM International, West Conshohocken, PA.

Tanyu, B., Benson, C., Edil, T., and Kim, W. (2004), Equivalency of Crushed Rock and Three Industrial By-Products Used As a Working Platform During Pavement Construction, *Transportation Research Record*, *Paper Number: 04-3105,* Transportation Research Board, National Research Council, Washington, DC. (in press for publication in the *Transportation Research Record*).

Thompson, M. R. (1999), "Hot Mix Asphalt Overlay Design Concepts for Rubblized PCC Pavements", *Transportation Research Board*, 78th Meeting, Washington D.C.

Tutumluer, E. and Thompson, M. R. (1997), "Anisotropic Modeling of Granular Bases in Flexible Pavements", *Transportation Research Record*, 1577, 18-26.

Ueshita, K. and Meyerhof, G. G. (1967), "Deflection of Multilayer Soil Systems", *Journal of Soil Mechanics: Foundations Division*, ASCE, 93, 257-282.

WisDOT (1996), *Standard Specifications for Highway and Structure Construction*, State of Wisconsin, Department of Transportation.

WisDOT (1997), "Subgrade Design/Construction Process Review", *District 1 Final Report*, State of Wisconsin, Department of Transportation Publication.

WisDOT (2003), "Facilities Development Manual", *State of Wisconsin Department of Transportation*.

Witczak, M. W. (2003). "Harmonized Test Methods for Laboratory Determination of Resilient Modulus for Flexible Pavement Design, Vlo. 1: Unbound Granbular Materials, NCHRP Report, Transportation Research Board, Washington, D.C.

Yoder, E. J. and Witczak, M. W. (1975), "Principles of Pavement Design", *John Wiley and Sons Publication*, New York.

CHAPTER TWO

STRUCTURAL CONTRIBUTION OF GEOSYNTHETIC-REINFORCED WORKING PLATFORMS IN PAVEMENT STRUCTURE

2.1 INTRODUCTION

Common pavement construction practice on soft subgrade requires a working platform constructed of granular materials to support heavy equipment during construction. This granular working platform after construction also serves to support traffic during the design life of the pavement similar to a subbase. Reinforcing this granular layer with geosynthetics can permit reduction in its thickness resulting in potential cost savings (Montanelli et al. 1997). This benefit is particularly attractive in areas where granular pavement material sources are scarce and longer hauls are involved. Furthermore, when the reinforced working platform is used as a subbase layer under long-term loading conditions, less rutting of the pavement surface under repeated traffic loading can be expected due to the reduction in vertical strains on the subgrade resulting in longer service life (Perkins 1999).

The objective of this study was to quantify the stiffness of four different geosynthetics-reinforced granular layers used as working platforms during construction over soft subgrade and to evaluate their structural contributions to the pavement structures under service loads. Large-scale model experiment (LSME) programs on two-layer systems consisting of reinforced granular materials and a soft subgrade were conducted to evaluate how each of reinforced granular layers

deflects under repetitive loads simulating in-service traffic. One hypothesis of the study was that the improved structural capacity of the pavement structures by geosynthetic reinforcements could be identified in terms of elastic deflections and quantified by back-calculating elastic modulus from the LSME and the field FWD deflection data for each case.

2.2 MATERIALS

Three granular materials were used in the LSME and field experimental program: a typical granular backfill (Grade 2) and two crushed rocks referred to herein as “breaker run”. Grade 2 is commonly used as base course or backfill and consists of a crushed rock screened to a gradation criterion (Wisconsin 1997). Breaker run is typically defined as large-sized aggregate resulting from crushing of rock that is not screened or processed after initial crushing. The breaker run rock and Grade 2 were retrieved during re-construction of a portion of Wisconsin State Highway (STH) 60. Both are derived from Cambrian dolostone in southern Wisconsin.

Particle size characteristics and other physical properties of the materials are summarized in Table 2.1. All of the materials are coarse-grained and classified as well-graded gravel (breaker run) and sand (Grade 2) in the Unified Soil Classification System (USCS). However, the gravel nomenclature is retained herein because of its common usage. Grade 2 is essentially insensitive to compaction water content. Breaker run is assumed also to be insensitive to water content because of

Table 2.1. Properties of Grade 2 and breaker run in LSME and field tests.

Material	Specific Gravity	Soil Fraction[a] (%)				USCS Symbol	Maximum Dry Unit Weight[b] (kN/m^3)	CBR
		Cobble	Gravel	Sand	Fines			
Grade 2	2.65	0	45	47	8	SW	22.6	33
Breaker Run (LSME)	NM[c]	23	49	25	3	GW	NM[c]	80[d]
Breaker Run (Field)	NM[c]	0	30	65	5	GW	NM[c]	80[d]

[a] Soil faction refers to the fraction of breaker run smaller than 75 mm (both breaker runs contained cobbles larger than 75 mm).
[b] Compaction per ASTM D 698.
[c] NM = not measured.
[d] Assumed CBR.

less fines (i.e., 3% to 5%) than Grade 2 (i.e., 8%). A compaction test could not be conducted on the breaker run because of its large particle size.

Four different geosynthetics (a geogrid, a woven geotextile, a non-woven geotextile, and a drainage geocomposite) were used in the study. Properties of geosynthetics used in this study are summarized in Table 2.2. Conventionally geocomposites are used primarily for drainage, but the contribution of the geocomposite as a reinforcing element was the focus of this study. These geosynthetics were used in a field demonstration program at STH 60 and therefore were also used in the laboratory investigation.

2.3 LARGE-SCALE MODEL EXPERIMENT (LSME)

The LSME test is a test apparatus for evaluating deflections during cyclic loading of a prototype-scale pavement structure (or parts of it) in a manner that replicates field conditions as closely as practical. A schematic of the LSME is shown in Fig. 2.1. A loading frame, actuator, and plate are used to simulate wheel loads. A detailed description of the apparatus can be found in Tanyu et al. (2003).

2.3.1 Subgrade and Pavement Profile

The subgrade and pavement profile tested in this study consisting of five layers is shown in Fig. 2.1 including a geosynthetic reinforcement layer, and a layer of test material (granular subbase material of varying thickness). Base course and asphalt were not included in the profile because the objective was to evaluate defle-

Table 2.2. Properties of geosynthetics used in LSME and field tests.

Geosynthetic Type	Property	Test Method	Values[g] (XMD)
TENAX MS™ 724[a] Geogrid	Thickness	ASTM D 5199	NM[h]
	Mass per Unit Area	ASTM D 5261	253.1 g/m^2
	Aperture Size[e]	NA[f]	32 (45) mm
	Peak Tensile Strength	GRI-GG1	17.2 (16.0) kN/m
	Yield Point Elongation	GRI-GG1	20 (11) %
	Offset Tangent Modulus	ASTM D 4595	88.3 (115.0) kN/m
AMOCO Style 2006[b] Woven Geotextile	Thickness	ASTM D 5199	0.7 mm
	Mass per Unit Area	ASTM D 5261	268.2 g/m^2
	Wide Width Tensile	ASTM D 4595	35.3 (42.3) kN/m
	Wide Width Elongation	ASTM D 4595	26 (19) %
	Offset Tangent Modulus	ASTM D 4595	147.9 (292.2) kN/m
AMOCO Style 4553[c] Non-woven Geotextile	Thickness	ASTM D 5199	2.7 mm
	Mass per Unit Area	ASTM D 5261	315.6 g/m^2
	Wide Width Tensile	ASTM D 4595	14.5 (21.8) kN/m
	Wide Width Elongation	ASTM D 4595	72 (57) %
	Offset Tangent Modulus	ASTM D 4595	34.0 (36.8) kN/m
TENAX Tendrain[d] Drainage Geocomposite	Thickness	ASTM D 5199	12.7 mm
	Mass per Unit Area	ASTM D 5261	1700.6 g/m^2
	Tensile Strength	ASTM D 4595	50.9 (54.4) kN/m
	Tensile Elongation	ASTM D 4595	57 (34) %
	Offset Tangent Modulus	ASTM D 4595	675.0 (200.0) kN/m
	Hydraulic Conductivity[e] at i = 0.1, σ_v = 720 kPa	NA[f]	25,000 m/day

[a] Biaxial oriented polypropylene.
[b] Polypropylene slit-film.
[c] Polypropylene needle punched.
[d] Tri-planar polyethylene geonet with non-woven polypropylene geotextiles.
[e] As reported by the manufacturer.
[f] NA=no standard method available.
[g] Machine direction (XMD=cross-machine direction).
[h] NM = not measured.

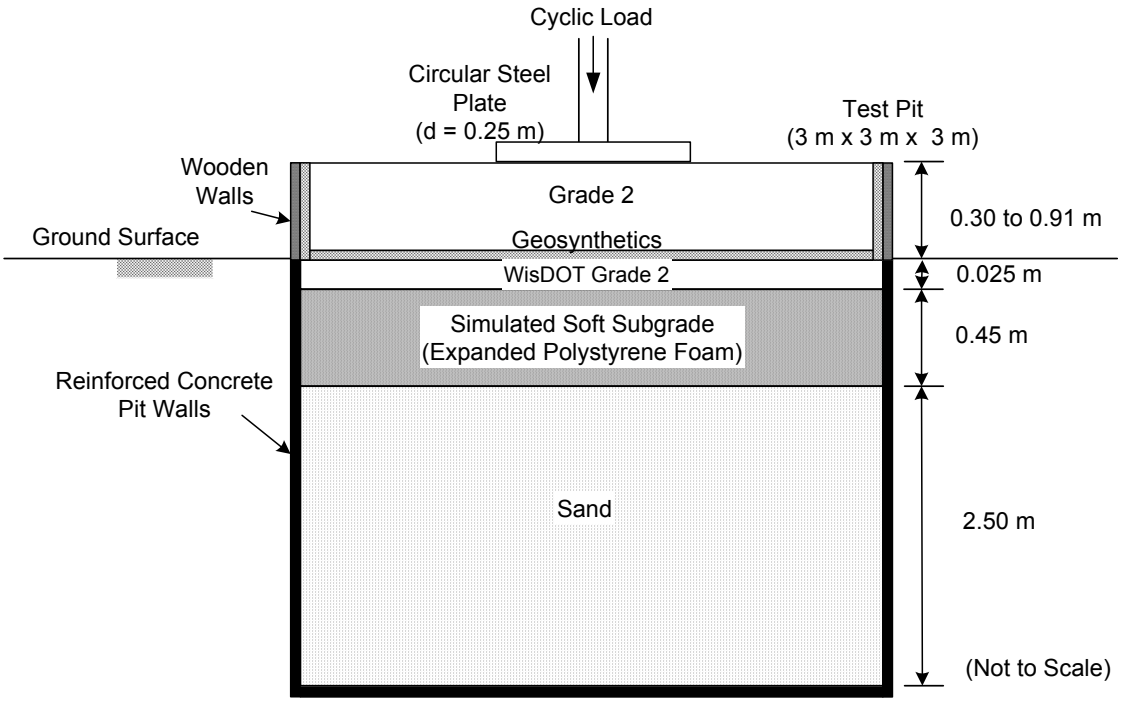

Fig. 2.1. Schematic cross section of large-scale model experiment (LSME).

ction of the geosynthetic-reinforced subbase under traffic loads during the service life of the pavements. The expanded polystyrene (EPS) foam with a similar stress-strain behavior as a typical soft subgrade soil was used to simulate a poor subgradein lieu of soft fine-grained soil (Tanyu et al. 2003).

Each lift of Grade 2 was compacted until the dry unit weight exceeded 95% of the maximum dry unit weight defined by the standard Proctor test (Table 2.1). Breaker run was compacted to the same dry unit weight (20.0 kN/m^3) used at the field control site (see subsequent discussion). Because of their insensitivity to water content during compaction, the Grade 2 and breaker run were placed in the LSME at their existing water content.

2.3.2 Loads and Deflections

Testing materials were subjected to two stages of repetitive loading: (i) higher intensity loading with small number of cycles (i.e., 1,000) simulating heavy truck traffic directly over the working platform during construction and (ii) lower intensity loading with large number of cycles (i.e., 10,000) simulating vehicular traffic on the finished pavement.

The second stage of loading (i.e., the lower intensity loading that is of primary concern for this phase of the study) was selected to simulate the stress induced at the working platform level by the surface vehicular traffic load. The induced load was calculated to be approximately 20% of the applied load on the surface of the pavement for a typical pavement structure (i.e., 140 kPa stress due to a 7 kN wheel

load) (Tanyu et al. 2003). Load was applied using a haversine load pulse consisting of a 0.1-s load period followed by a 0.9-s rest period, the same load pulse specified in the small-scale laboratory resilient modulus test.

Resilient modulus of the working platform materials were obtained by inversion from KENLAYER using the data obtained from the LSME. In the inversion analysis, moduli of the working platform layers were assumed to follow the non-linear elastic k-σ_b model:

$$M_r = k_1 \sigma_b^{k_2} \quad (2.1)$$

where k_1 and k_2 are empirical constants and σ_b is the bulk stress. This model has been shown to be a satisfactory model for a wide range of granular materials (Perkins 2001).

Vertical deflections of the pavement profile were measured directly underneath the loading plate and at distances of 300, 450, and 650 mm away from the centerline of the actuator. Position transducers were used to measure the deflections during each loading cycles (Tanyu et al. 2003).

2.3.3 Instrumentation

The displacements in geosynthetics were measured using calibrated linear variable differential transformers (LVDTs), which had a stroke of ± 50 mm and a

nominal sensitivity of 1.5 V/V, with external signal conditioning. The end of the steel extension wire in the LVDT unit was attached to the geosynthetic at 0 mm, 130 mm, 255 mm, and 510 mm from the loading center in the cross machine direction.

Strain levels in the geosynthetic were measured with a series of resistance type strain gages attached on the upper and lower surfaces of the geosynthetic. The strain gage length of 6.35 mm and width of 3.18 mm (Micro-Measurement Division EP-08-250BG-120) were used for the geogrid and the drainage geocomposite, while 50.8 mm long and 4.78 mm wide strain gages (EP-08-20CBW-120) were used for the geotextiles. Strain levels in cross-machine direction of the geosynthetic were measured at five different locations from the center of the loading plate: 0 mm, 130 mm, 255 mm, 380 mm, and 510 mm. The procedures described in the literature were followed in mounting the strain gages to different types of geosynthetics (Farrag 1999, Chew et al. 2000, Hayden et al. 1999, Kim 2003).

2.4 FIELD EXPERIMENT (STH 60)

Field tests were conducted on a 312-m long pavement segment of STH 60 between Lodi and Prairie du Sac, Wisconsin that contains twelve test sections with different pavement profiles. Edil et al. (2002) provide a detailed description of these test sections. Five of these test sections were evaluated in this study. Four were constructed using 0.3-m thick breaker run reinforced with the four geosynthetics described above as the working platform. One section at the east end of the test site was constructed using 0.84-m thick breaker run without geosynthetic

reinforcement as control section. There was no Grade 2 section reinforced with geosynthetics. The subgrade at the test site consists of lean silt (ML) or lean clay (CL) as described by Edil et al. (2002).

The geosynthetic materials were spread over the subgrade in the machine direction parallel to the traffic lanes and breaker run was placed over the geosynthetic in a single lift (i.e., 0.30 m) using a loader, while the unreinforced breaker run in the control section was placed in 0.15-m-thick lifts and compacted. All sections had a 0.13-m-thick AC layer and a 0.25-m-thick base course consisting of 0.11-m Grade 2 and 0.14-m salvaged asphalt, which has essentially the same properties as Grade 2. Deflections in each test section were measured using Falling Weight Deflectometer (FWD) since STH60 was opened to the traffic *(*2002*)*.

2.5 ANALYSIS

2.5.1 Back-calculation of Elastic Modulus from LSME

KENLAYER (Huang 2004) was used to back-calculate the elastic modulus of the geosynthetic-reinforced subbases from the measured surface deflections in the LSME. The simulated soft subgrade was assumed to be linearly elastic, whereas the elastic modulus of the subbase was assumed to follow the elastic power function given in Eq. 1.1. The elastic deflections used were derived from the total deflections (elastic and plastic) measured in the LSME by subtracting the accumulated plastic (non-recoverable) deflections from the total deflections and used in KENLAYER.

To assess the influence of the effective thickness of the stiffened portion of the reinforced subbase by the geosynthetic inclusion, the subbase was divided into sublayers of several thicknesses in the KENLAYER analysis. The parameter k_2 varies in a very narrow range for granular materials. Thus, k_2 was fixed at 0.50 for Grade 2 using the value obtained from the resilient modulus test conducted per AASHTO T294-94 (Tanyu et al. 2003), while k_2 was assumed to be 0.45 for the breaker run. The parameter k_1, which varies over a broad range, was adjusted for the reinforced sublayer of the subbase containing the geosynthetic until the measured and the elastic deflections predicted by KENLAYER matched. The k_1 that provided the matching deflections was assumed to be the operative k_1 of the geosynthetic reinforced sublayer of the subbase. The other sublayers of the subbase that did not contain the reinforcing geosynthetic were assumed to have a k_1 as obtained from the LSME tests performed on the unreinforced Grade 2 and breaker run, respectively.

Analyses were performed to determine the thickness of unknown reinforced sublayer of the subbase, in which the thickness of the reinforced sublayer was varied from 25 to 200 mm. For sublayer thickness larger than 100-mm, the elastic modulus becomes nearly constant (Kim 2003). Therefore, the 100-mm-thick reinforced sublayer of the subbase was assumed in subsequent analyses.

2.5.2 Back-calculation of Elastic Modulus from FWD Test

The subbase elastic modulus in the field was back-calculated from the measured FWD deflections using the layered elastic analysis program MODULUS (Texas Transportation institute 1991). A four-layer system (asphalt concrete, base course, subbase, and subgrade) was used for the back-calculation model. The geometric mean temperature on the surface of AC layer at the time of FWD testing was used to obtain the modular range for the AC layer in MODULUS input. Elastic moduli assigned to each pavement layer were adjusted iteratively until the measured and predicted deflections matched within an accepted tolerance (Kim 2003).

Once the field subbase elastic moduli were back-calculated using MODULUS, an additional analysis was conducted with KENLAYER to determine the range of bulk stresses and vertical strains operative in the subbase layer in the field. The back-calculated elastic moduli with MODULUS were used as input in bulk stress analysis. The bulk stress and vertical strain at mid-depth of each layer were assumed to be representative of the operative conditions in the field.

2.6 RESULTS AND DISCUSSION

2.6.1 LSME Tests

2.6.1.1 Elastic Deflection

Elastic deflections (δ_e) under the loading plate of the LSME as a function of the number of load cycles are shown in Fig. 2.2 for Gravel 2 gravel subbase with or without reinforcement with geosynthetics. Elastic deflections accumulate monotoni-

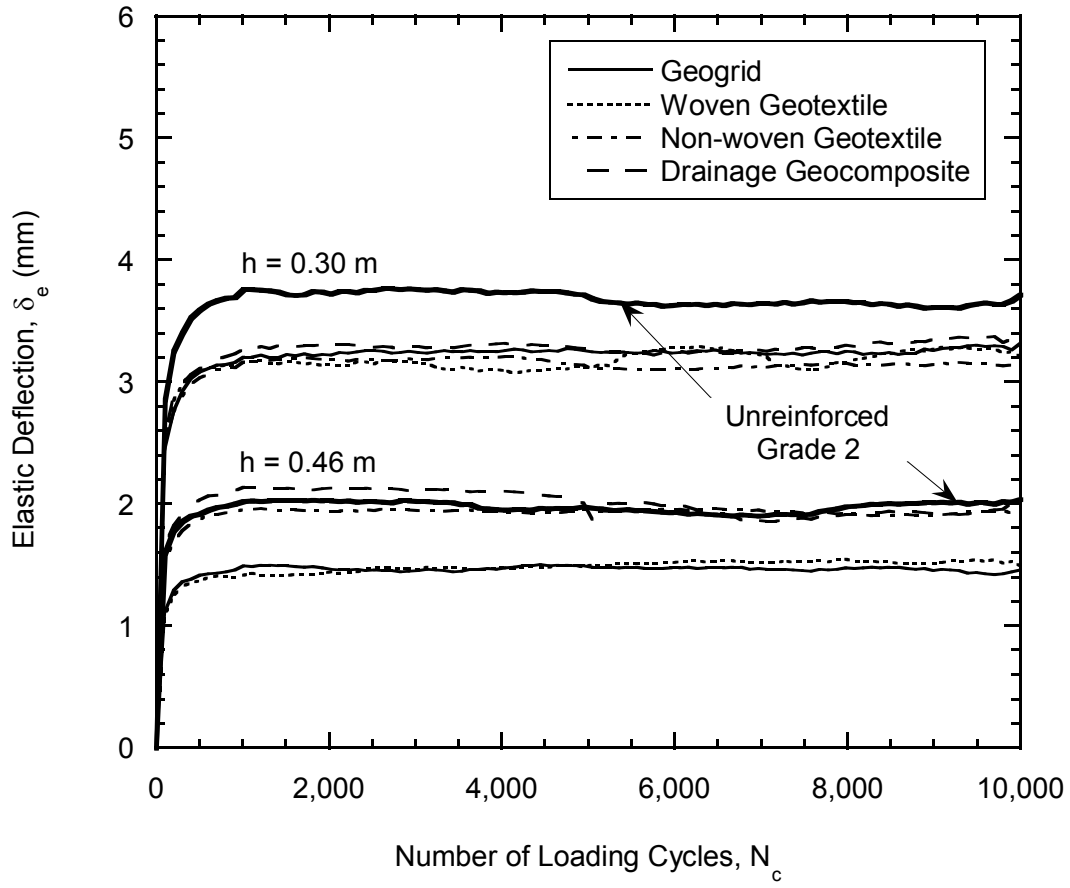

Fig. 2.2. Comparison of elastic deflection under the loading plate of the LSME as a function of number of load cycles for subbases constructed with Grade 2 reinforced with geosynthetics having a thickness (h) of 0.30 m and 0.46 m.

cally during the tests and quickly increase at the onset of the loading cycle, with the greatest rate of accumulation within the first 100 cycles. The deformation rate then decreases as the number of load cycles increase and a steady state condition is reached after approximately 1,000 cycles. In addition, the elastic deflections are smaller for the thicker layer for all loading cycles (i.e., approximately half of the deflections measured in 0.30-m thick). Overall deflections are less than 4 mm.

For the thinner subbase (0.30 m), the elastic deflections under the loading plate are smaller for the geosynthetic-reinforced Grade 2 compared to that for the unreinforced subbase. The average deflection of the last 500 cycles for the reinforced subbases is lower by approximately 8% to 12%. However, no significant effect of the geosynthetic type on the elastic deflection is observed for the 0.30-m-thick layer. On the other hand, as the subbase becomes thicker (0.46 m), the average elastic deflection decreases by 24% and 27% for the geogrid- and the woven geotextile-reinforced subbases respectively, while no reduction in the elastic deflection is shown for the non-woven geotextile and the drainage geocomposite reinforced subbases. The reinforcement function of the drainage geocomposite is probably realized through the non-woven filter geotextiles that are continuous and in contact with the soil rather than the discontinuous internal geonet panels, thus resulting in a behavior similar to that of the non-woven geotextile reinforcement. The inextensible geosynthetic-reinforced (i.e., the geogrid and the woven geotextile in this study) subbases continue to reduce the elastic deflections as the layer thickness increases. This behavior is consistent with the observations reported by others (Fannin and Sigurdsson 1996, Leng and Garb 2002).

The deflection basins in Fig. 2.3a illustrate the relative stiffness of the geosynthetic-reinforced subbases. Less but similar deflections are obtained from the geosynthetic-reinforced subbases compared to the unreinforced subbase. Similar observations in reduced deflection were reported by others (Haas et al. 1988, Kinney et al. 1998). The gauge strain and displacement in the reinforcing geosynthetic under loading plate during 10,000 load cycles is shown in Fig. 2.3b for geosynthetic-reinforced subbases. Although less deflection is obtained from each geosynthetic-reinforced subbase, their load-deformation behaviors are differentiated. Tensile gauge strains of 2.2% to 2.4% with tensile movement of 0.02 to 0.04 mm beneath the loading plate after 10,000 load cycles are measured for the geogrid and the woven geotextile-reinforced subbases. Almost no strains with much smaller movements are observed in the non-woven geotextile and the drain geocomposite reinforced layers, which could be due to the difference in polymers, the structure, the gauge location, and/or bonding between the geosynthetic and the granular subbase. For the subbases reinforced by the geogrid and the woven geotextile, the slight compression strains are observed at a radial distance between 130 mm and 380 mm from the loading center and diminished rapidly with distance. The similar pattern of strain distribution was observed by Perkins (1999) for a crushed stone base course reinforced with the woven geotextile and the geogrid.

The shape of the defection basin was flatter for the thicker layer (0.46 m) and also for the subbases reinforced with the geogrid and the woven geotextile compared to that for the unreinforced layer (Kim 2003). The more gradual distribution and lower elastic deflection beneath the center of the loading plate

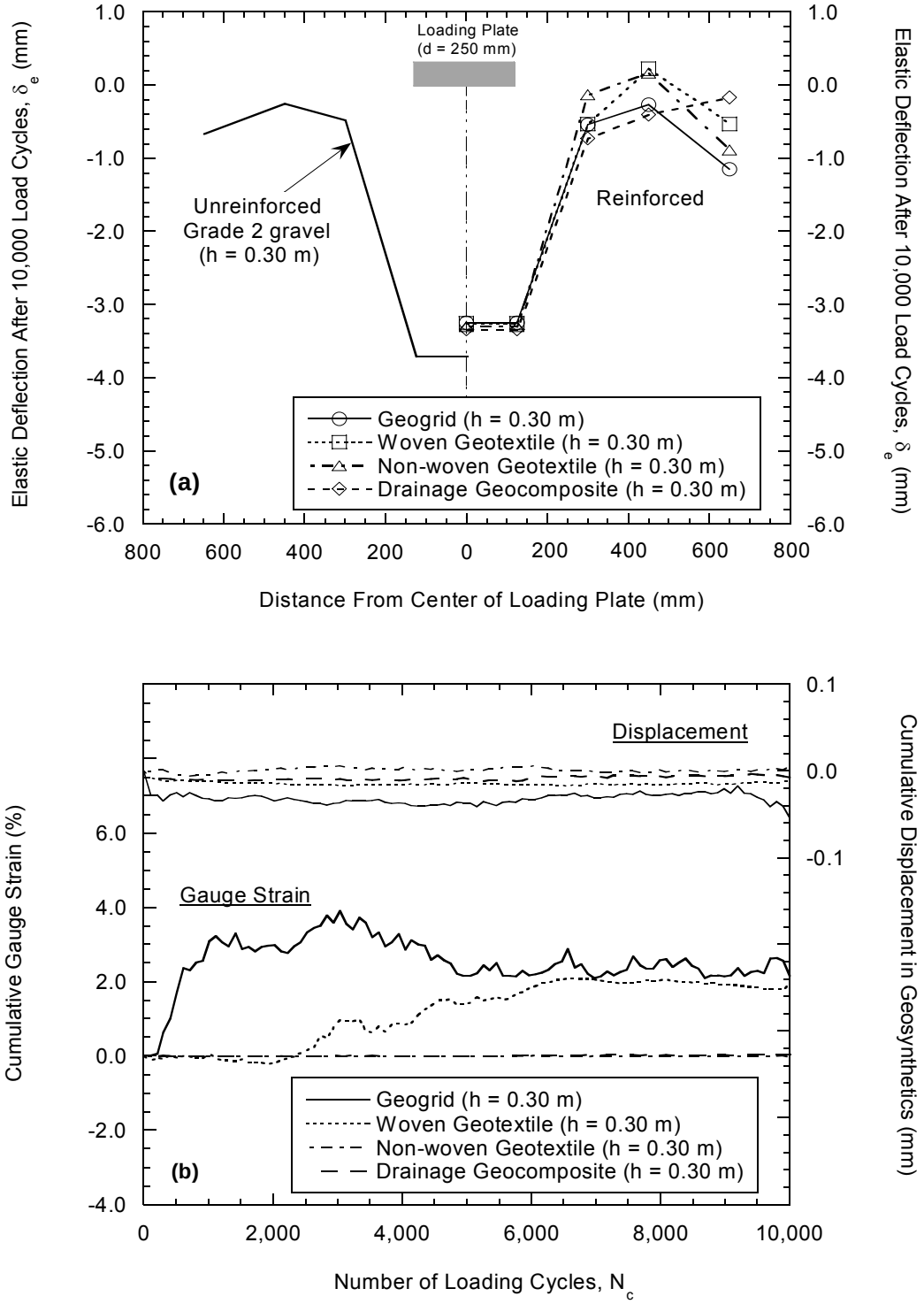

Fig. 2.3. Elastic deflection basins for geosynthetic-reinforced subbases after 10,000 load cycles in the LSME (a), and gauge strain and displacement in the geosynthetic under loading plate as a function of number of load cycles (b), when the thickness is 0.30 m (i.e., h = 0.30 m).

observed for the reinforced subbases imply that the geosynthetic-reinforced subbases are relatively stiffer than the unreinforced layer. As the subbase becomes thicker, the elastic deflection decreased due to the additional stress distribution and corresponding reduction in strain in a thicker layer (Tanyu et al. 2003). As the subbase becomes thicker, the strain in the geosynthetic located at the bottom of the subbase decreased with decreasing elastic deflections (Kim 2003). This may imply that additional surface permanent deflections are needed to mobilize the geosynthetic reinforcement when using a thicker subbase reinforced with geosynthetics. This tendency is consistent with the observations by others (Perkins 1999, Collin et al. 1996). The only exception occurred with the 0.46-m-thick subbases reinforced with the non-woven geotextile and the drainage geocomposite for the same reason as described previously.

The deflection basins also show the region of influence of the loading plate (Fig. 2.3a). The elastic deflection diminished rapidly with distance, and is very small (less than 0.6 mm) for all geosynthetics at a distance of 300 mm from the center of the loading plate (175 mm from the edge of the loading plate). Therefore, all subsequent comparisons are based on deflections directly under the loading plate.

2.6.1.2 Back-Calculated Elastic Moduli from LSME Tests

The back-calculated elastic moduli corresponding to the average elastic deflection of the last 500 load cycles for each geosynthetic-reinforced Grade 2 subbase in the LSME are shown in Fig. 2.4 as a function of bulk stress for the two subbase thicknesses. Two approaches were taken to back-calculate the elastic

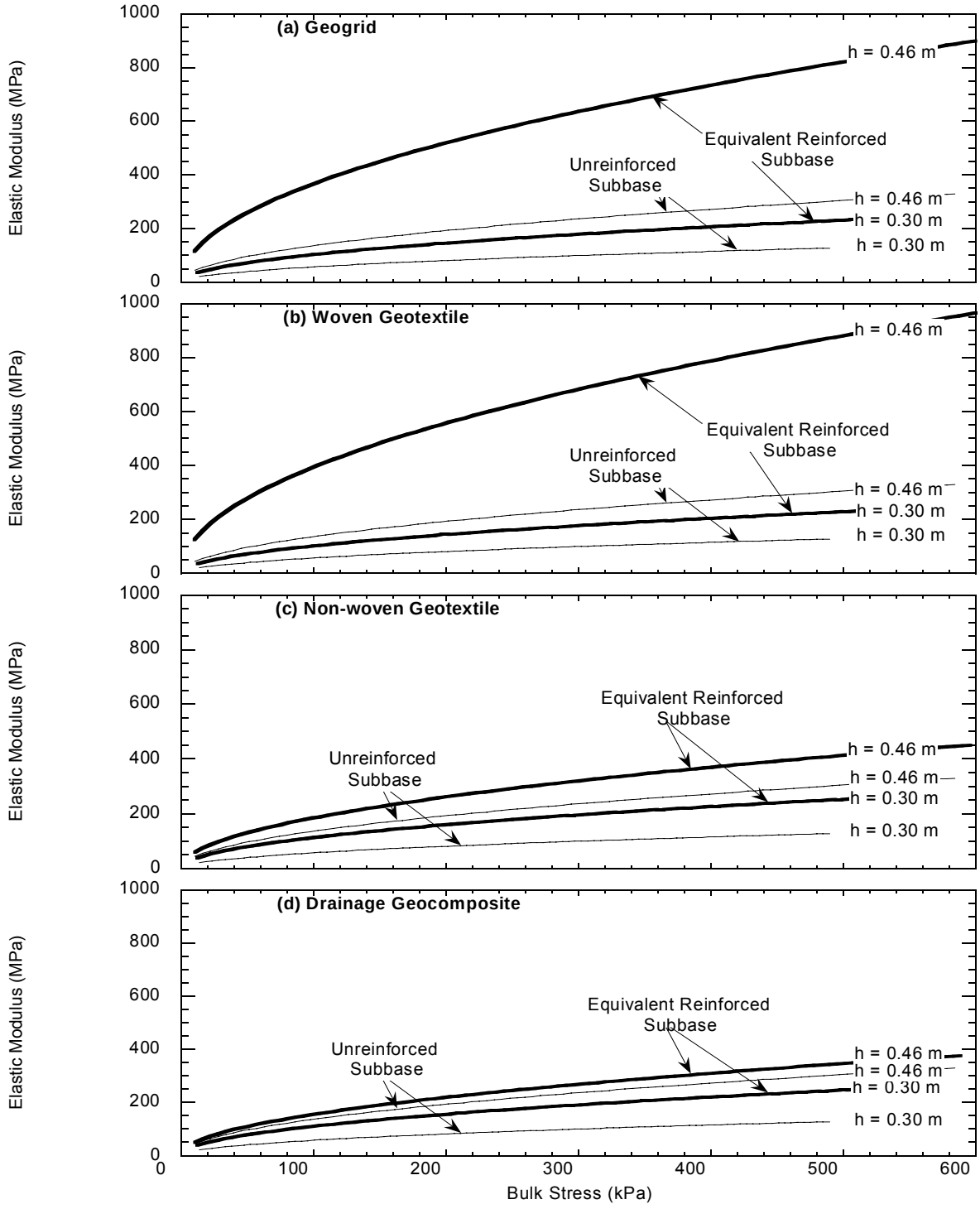

Fig. 2.4. Comparison of back-calculated elastic moduli for geogrid (a), woven geotextile (b), non-woven geotextile (c), and drainage geocomposite (d) reinforced subbases in the LSME after 10,000 load cycles (h = subbase thickness).

modulus for each reinforcing material using KENLAYER analysis described previously: (1) treat the entire subbase as a single reinforced layer with an equivalent improved modulus (referred to as “equivalent reinforced subbase”) and (2) divide the subbase into sublayers treating only the bottom sublayer as a single reinforced sublayer with an improved modulus and the sublayers above as unreinforced sublayers (referred to as “reinforced sublayer”). In the second approach, the reinforced sublayer was assumed to have a thickness of 100 mm whereas unreinforced sublayers typically 50 mm.

The back-calculated elastic modulus using the “equivalent reinforced subbase” increases appreciably with increasing bulk stress and is higher for the reinforced subbases compared to the unreinforced subbase of equal thickness. Furthermore, the back-calculated elastic modulus in the LSME is sensitive to the thickness of the subbase layer (h) being evaluated due to the effect of strain amplitude that occurs in layers of different thickness as demonstrated by Tanyu et al. (2003).

The back-calculated composite moduli of the “reinforced sublayer” following the second approach also vary depending on subbase thickness, more significantly for the geogrid and the woven geotextile (i.e., the less extensible geosynthetics) than for the non-woven geotextile or the drainage geocomposite (i.e., more extensible geosynthetics). This is consistent with the geosynthetic movement and strain data such as given in Fig. 2.3.

The average k_1 obtained in the back-calculation using KENLAYER for the “equivalent reinforced subbase” are presented in Table 2.3 along with the k_1 ratio for

Table 2.3. Average k_1 and k_1 ratio for geosynthetic-reinforced Grade 2 subbases from the LSME.

Geosynthetic Reinforcement	Subbase Thickness, h (m)	k_1 (MPa)		$k_{1\text{-reinforced}}$[b] / $k_{1\text{-unreinforced}}$[b]	
		Equivalent Reinforced Subbase	Reinforced Sublayer[a]	Equivalent Reinforced Subbase	Reinforced Sublayer
None	0.30	15.2	15.2	1.0	1.0
	0.46	35.9	35.9	1.0	1.0
Geogrid	0.30	29.8	25.2	2.0	1.7
	0.46	96.5	93.9	2.7	2.6
Woven geotextile	0.30	29.0	25.0	1.9	1.7
	0.46	103.4	108.5	2.9	3.0
Non-woven geotextile	0.30	26.6	22.8	1.8	1.5
	0.46	48.6	41.5	1.4	1.2
Drainage geocomposite	0.30	25.5	22.4	1.7	1.5
	0.46	40.7	37.6	1.1	1.1

[a] Average k_1.

[b] k_1 values essentially correspond to the modulus at the same bulk stress.

each geosynthetic reinforced subbase to that of the unreinforced subbase. Also given in Table 2.3 are the k_1 computed for the "reinforced sublayer" and the corresponding k_1 ratios. These can be used if multiple layers of geosynthetic are used in characterizing the local reinforcement in each thin sublayer of the subbase containing the geosynthetic.

For the 0.30-m thick reinforced subbases, the k_1 ratio ranges from 1.7 to 2.0 and 1.5 to 1.7 for the "equivalent reinforced subbase" and for the "reinforced sublayer" approaches, respectively, while for the thick subbases, the ratio ranged between 1.1 and 2.9 for the "equivalent reinforced subbase" and 1.1 and 3.0 for the "reinforced sublayer". The k_1 ratio from the "reinforced sublayer" gives equal or slightly lower k_1 (i.e., modulus) compared to the "equivalent reinforced subbase" with marginal ranges, except in one case, that is, for the 0.46-m thick subbase with the woven geotextile. The difference becomes greater in the thinner (i.e., 0.30 m) layer of subbase.

2.6.2 Field Tests

To verify the increase in the elastic modulus by geosynthetic subbase reinforcement in the field, a series of FWD tests on the test sections built at the STH 60 were conducted between October 23, 2000 and October 21, 2002. The seasonal variations of the asphalt concrete surface temperatures and the associated surface deflections during FWD tests are shown in Fig 2.5a. The fact that bitumen softens as its temperature increases and stiffens as it decreases leads to transmittal of

different stresses in the underlying unbound granular layers under the same applied load. The stiffness of the granular layers is stress dependent, but also changes with asphalt temperature.

Based on the deflections from the FWD tests, the back-calculated subbase elastic moduli for each section at 40-kN load that generates stresses at the subbase layer that are the closest to those applied in the LSME are shown in Fig. 2.5b. The reasons for the back-calculated modulus differences are not clearly known but are probably due to the stiffness of the asphalt concrete layer in relation to that of the overall pavement structures. The subbase elastic moduli are lower for the non-woven geotextile and the drainage geocomposite sections, and are slightly higher for the woven geotextile and the geogrid reinforced sections. The degree of the subbase elastic modulus affected by the type of the geosynthetic on the breaker run in the field is consistent with that observed from the LSME tests on the reinforced Grade 2. Overall the elastic moduli from the 0.30-m thick geosynthetic-reinforced subbases in the field test sections are comparable to each other with marginal ranges and to that from the thicker (0.84 m) unreinforced breaker run control section.

Seasonal variations in back-calculated elastic modulus were observed (Kim 2003). The geometric spatial mean of elastic moduli in the field geosynthetic-reinforced sections were initially high after the completion of the pavement structure before the roadway opened to traffic (October, 2000); subsequently, the moduli of the reinforced sections decreased but did not vary significantly over the next 2 years (Kim 2003). Initially pavement layers had probably not fully interacted with each

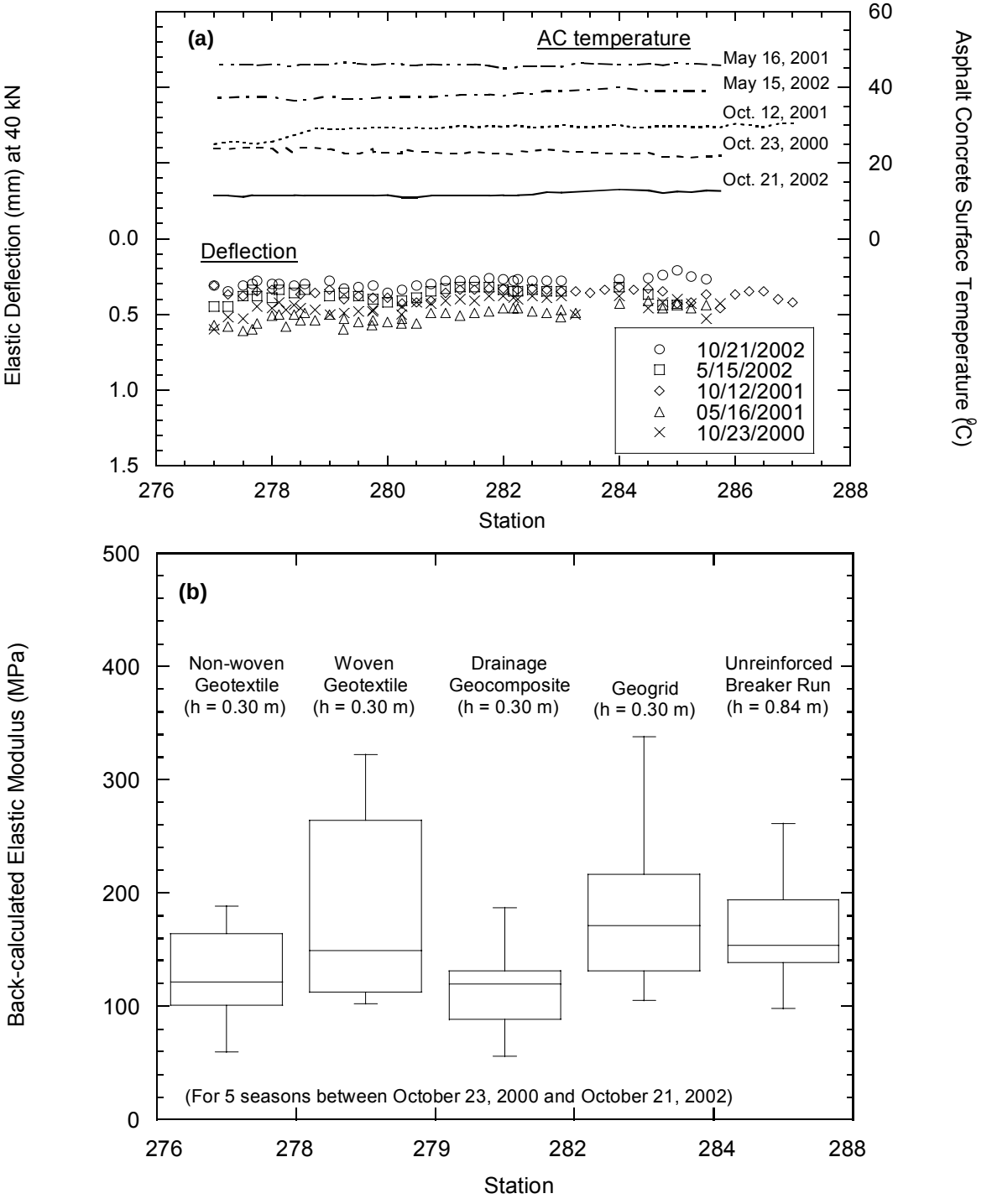

Fig. 2.5. Elastic deflection corresponding the asphalt concrete temperature (a) and back-calculated subbase moduli (b) from FWD tests conducted between October 23, 2000 and October 21, 2002 at STH 60 (h = subbase thickness).

other under the small amount of traffic loads accumulated. Table 2.4 gives the arithmetic average of the geometric spatial mean elastic moduli over the last 4 measurement events (along with the range of individual values) as well as the corresponding field breaker run reinforcement factors. The equivalent reinforced subbase moduli and reinforcement factors for the Grade 2 as obtained from the LSME are also given in Table 2.4.

2.6.3 Comparison of Field and Laboratory Behavior

Because different granular materials were used in the geosynthetic-reinforced subbases of the LSME and the field test sections (Grade 2 and breaker run, respectively), a direct comparison of the laboratory and the field moduli may not be appropriate. However, the grain size distribution of the soil fraction of the breaker run used in the field is comparable to the Grade 2 (Table 2.1) and the cobbles and boulders in the breaker run were not placed directly over the geosynthetics in the field. Therefore, the interaction of each material with the geosynthetics, except perhaps the geogrid (because of its apertures), can be considered comparable. Furthermore, the effect of geosynthetics can be expressed as a normalized reinforcement factor (i.e., ratio of moduli of the geosynthetic-reinforced and the unreinforced subbases) in the LSME and the field and can be compared with each other. Because test results for the unreinforced breaker run is available both in the LSME and the field (although the breaker run is slightly different in each case), a comparison of the back-calculated moduli from each can be made to evaluate the

Table 2.4. Comparison of unreinforced and geosynthetic-reinforced breaker run subbasemoduli and reinforcement factor (h =subbase thickness).

	M_r (MPa)					Reinforcement Factor ($M_{r\text{-reinforced}}$ / $M_{r\text{-unreinforced}}$)			
	Unreinforced Subbase (h = 0.30 m)	Geosynthetic-Reinforced Subbase (h = 0.30 m)							
		Geogrid	Woven Geotextile	Non-woven Geotextile	Drainage Geocompsite	Geogrid	Woven Geotextile	Non-woven Geotextile	Drainage Geocompsite
FWD (Breaker Run)	93[b, c] (88-106)[b, d]	163[c] (135-186)[d]	133[c] (115-160)[d]	135[c] (114-155)[d]	110[c] (98-120)[d]	1.8[c] (1.5-2.0)[d]	1.5[c] (1.2-1.8)[d]	1.5[c] (1.1-1.8)[d]	1.2[c] (1.1-1.3)[d]
LSME[a] (Grade 2)	40	78	76	70	67	2.0	1.9	1.8	1.7

[a] From equivalent reinforced subbase analysis for Grade 2 subbase.
[b] Extrapolated from 0.84 m to 0.30 m thickness at the mean field bulk stress of 43 kPa.
[c] Based on the geometric spatial and arithmetic temporal means excluding October 2000 data
[d] Based on the minimum and maximum values excluding October 2000 data.

relevance of the LSME to the field prior to comparing the reinforcement factors. Another complication arises because of the different thicknesses of the geosynthetic-reinforced breaker run subbases and the unreinforced subbase in the field (i.e., 0.30 m and 0.84 m, respectively) to generate a field reinforcement factor. These two issues are addressed before a comparison of the laboratory and the field reinforcement ratios is made.

The back-calculated elastic moduli for the unreinforced LSME breaker run subbases (0.30-m, 0.46-m, and 0.91-m thick) and the unreinforced field breaker run subbase (0.84-m thick) using KENLAYER and MODULUS, respectively, were calculated as a function of bulk stress. The FWD moduli for the breaker run subbase were consistently higher than the LSME moduli but reasonably close to the moduli for a subbase of comparable thickness in the LSME (Kim 2003). This finding is in general agreement with the results reported by others (Parker 1991, Tanyu et al. 2003). Because a reasonably close relationship is observed between the field and laboratory moduli for the unreinforced breaker run subbases of similar thickness (i.e., 0.84 m), a field modulus corresponding to an unreinforced breaker run subbase layer of 0.30 m thickness is estimated using the ratio of the LSME moduli of the 0.84-m and 0.30-m thick breaker run subbases at mid-depth of the layer, which was determined to be approximately 58% at the mid-depth at a mean field bulk stress of 43 kPa. Assuming a similar reduction occurs in the field as in the LSME due to decreasing thickness, the elastic modulus of a 0.30-m thick unreinforced breaker run subbase in the field is estimated as 58% of the back-calculated field modulus of the 0.84-m thick unreinforced breaker run subbase. This modulus for the 0.30-m thick

unreinforced breaker run subbase then is used in calculating a field reinforcement factor by dividing the corresponding moduli back-calculated for different 0.30-m thick geosynthetic-reinforced sections in the field with it.

The mean field reinforcement factors (along with the range of individual values) as given in Table 2.4 are compared with those from the LSME tests in Fig. 2.6. The highest reinforcement factor is from the geogrid-reinforced section and the least is from the drainage geocomposite section. The reinforcement factors from the LSME tests follow essentially the same ranking but they are a little higher than the field reinforcement factors. Two different but close granular materials were used in the laboratory and the field reinforced subbase sections and the LSME were performed at essentially constant room temperature and moisture and do not incorporate all factors operating in the field. Furthermore, the slightly higher reinforcement factor in the LSME may result from the low strength of the simulated subgrade (CBR $\leq$ 1) compared with that in the field.

2.7 PRACTICAL IMPLICATIONS

Pavement design following the new AASHTO guideline is going to incorporate elastic (resilient) modulus, which will be assigned to each layer in the pavement system. These moduli are then used to obtain layer coefficients for each layer and to produce a structural number (i.e., the product of the layer coefficient and thickness in inches of each layer) for flexible pavement design. The sum of the structural numbers contributed by each layer provides the composite structural

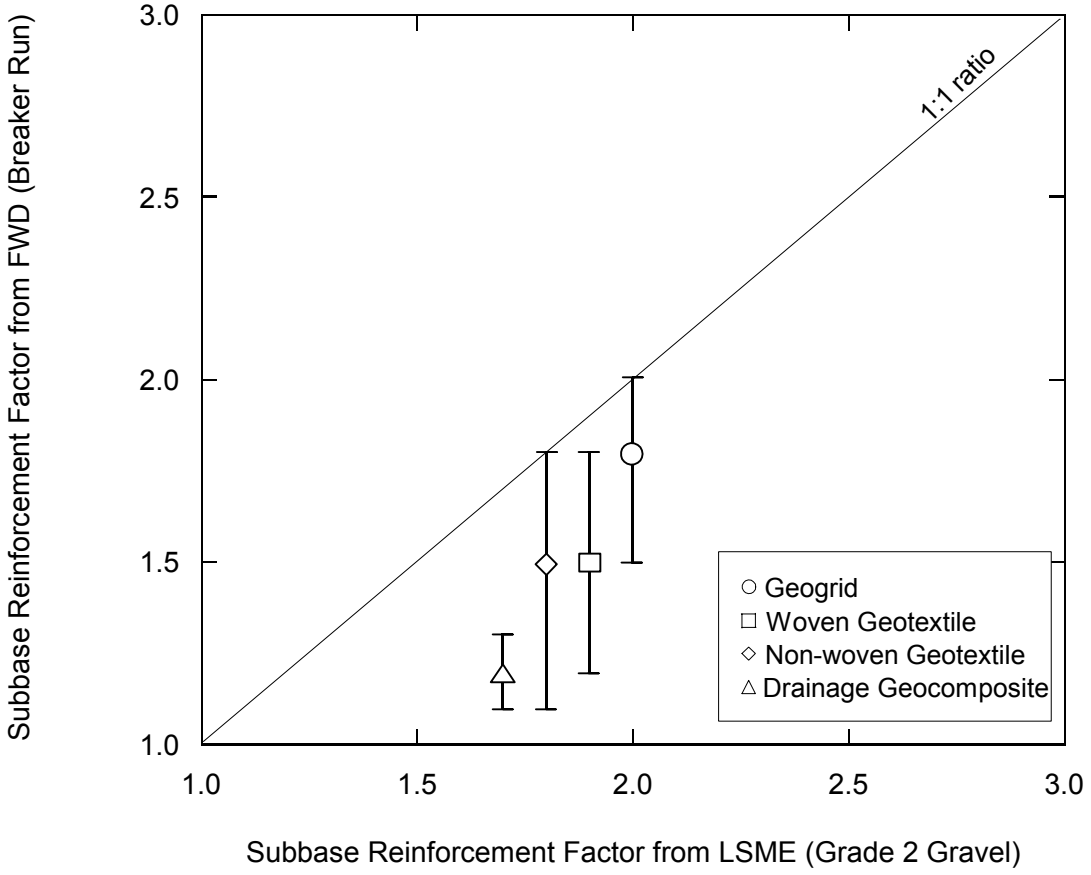

Fig. 2.6. Comparison of the reinforcement factor from LSME and FWD tests.

number that represents the entire flexible pavement structure. The layer coefficient for each layer is related to an elastic modulus using the equations developed by Rada and Witczak (1981). For granular subbase materials, the relationship is

$$a_3 = 0.227\log(M_r) - 0.839 \quad (2.2)$$

where a_3 is the layer coefficient and M_r (psi) is the elastic modulus for the granular subbase material. A geosynthetic-reinforced working platform that is placed as a construction aid can be treated as a subbase with an improved elastic modulus for the purpose of subsequent performance of the roadway under regular traffic loads. The reinforced layer elastic modulus for each geosynthetic can be obtained by multiplying the corresponding reinforcement factor with the elastic modulus at the mid-depth of the unreinforced subbase of equal thickness. These moduli then can be used to determine the corresponding layer coefficient in accordance with Eq. 2.2.

Based on this research, elastic moduli for the subbases constructed using granular materials similar to breaker run and having a thickness of 0.30 m and reinforced by the type of geosynthetics used in the current study can be estimated. This subbase thickness and the materials used in the current study are quite typical but by no means general. In estimating the reinforced layer moduli, the minimum values of the reinforcement factors within the range they vary, rather than their mean values are recommended as a conservative approach. For each geosynthetic, the ratio of the reinforced to unreinforced subbase layer coefficient from the LSME and

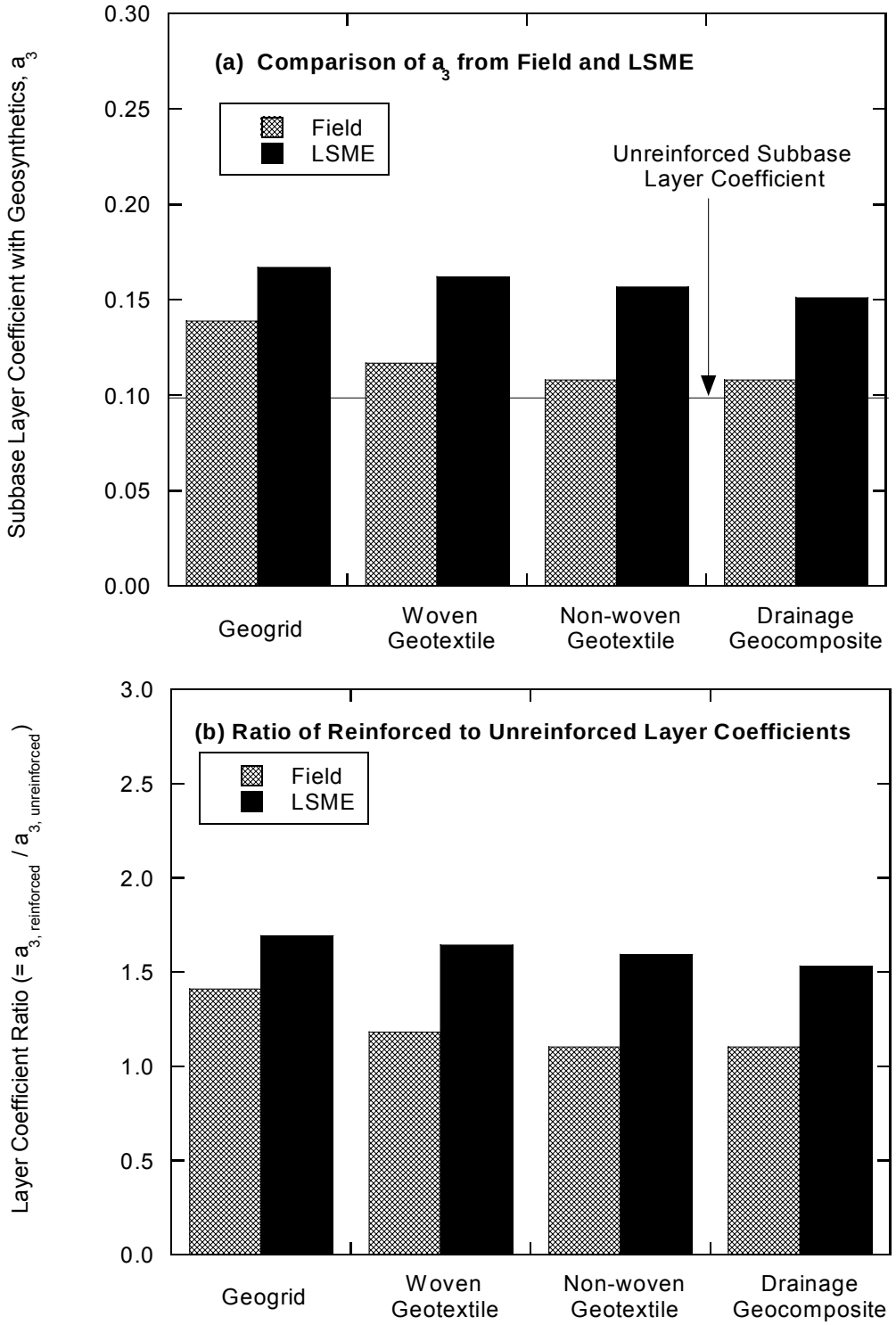

Fig. 2.7. Increased layer coefficient due to geosynthetic reinforcement (a) and the ratio of reinforced to unreinforced layer coefficients (b) in breaker run subbase layer.

field tests (using the minimum values) are shown in Fig. 2.7. The improvement in layer coefficients based on low-end field reinforcement factors are lower than those based on the LSME reinforcement factors and rather small for the nonwoven geotextile and drainage geocomposite (10%) and somewhat higher for the geogrid (40%) and for the woven geotextile (18%). However, overall these improvements cannot be considered very significant in terms of the contribution to the composite structural number. The contribution of the geosynthetic would be even less to the elastic improvement of the pavement system when the thickness of the subbase layer is greater than 0.30 m as shown in the LSME tests on 0.46-m thick reinforced subbase. The recommended layer coefficients and structural numbers for flexible pavements are summarized in Table 2.5 for various geosynthetic reinforcements placed in 0.3-m thick granular material similar to Grade 2.

For rigid pavements, a composite modulus of subgrade reaction is needed. It can be developed from these subbase moduli and an assumed soft subgrade modulus as explained earlier in Section 1.6.

2.8 SUMMARY AND CONCLUSIONS

The objective of this study was to quantify and evaluate the structural contribution of a geosynthetic-reinforced granular subbase layer that can be used as a working platform during construction over soft subgrade, to the pavement structure under service loads. The effect of geosynthetics was expressed as a normalized

Table 2.5. Recommended layer coefficients and structural numbers for flexible pavements with and without geosynthetic reinforced working platforms.

Design Element	Unreinforced	Geogrid	Woven Geotextile	Nonwoven Geotextile	Drainage Geocomposite
Working Platform Layer Coefficient, a_3	0.10	0.17	0.16	0.16	0.15
Structural Number, SN[a]	4.58	5.06	4.80	4.69	4.69
Increase in Structural Number (%)	-	11	5	3	3

[a] $SN = a_1D_1 + a_2D_2m_2 + a_3D_3 m_2$ where a_i is the layer coefficient of layer i, D_i is the thickness of layer i (inches), and m_i is the drainage modification factor.

reinforcement factor (i.e., a ratio of modulus of the geosynthetic-reinforced and the unreinforced subbases) and the layer coefficient ratio (LCR). The reinforcement factor and layer coefficient ratio for each geosynthetic-reinforced subbase layer in the LSME were checked with field data from falling weight deflectometer (FWD) tests.

The reinforcement factors from the LSME tests follow essentially the same ranking but they are a little higher than the field reinforcement factors. Based on the field FWD data, some variation of the reinforcement factors over time was observed because of seasonal effect. Working platforms reinforced with geosynthetics had smaller elastic deflections and larger elastic moduli than unreinforced working platforms having the same thickness. Reinforcement factors ranging from 1.2 to 1.8 were obtained in the field and 1.7 to 2.0 in the laboratory, with greater reinforcement factors for the less extensible geosynthetics (geogrid, woven geotextile) for a 0.3 m-thick granular working platform. Of the four geosynthetics tested, the geogrid resulted in the greatest increase in modulus.

Structural contributions of the working platforms were estimated by treating them as a subbase in the conventional AASHTO design method for flexible pavements with a layer coefficient and computing a structural number for the pavement system. Reinforcing the working platforms with geosynthetics resulted in increases in layer coefficients ranging from 50 to 70%. Similarly, increases in structural number for a typical pavement structure were realized ranging from 3 to

11% when all other factors were equal, with the largest increase in structural number obtained the geogrid was used a reinforcement.

The new Guide for Mechanistic-Empirical Pavement Design (NCHRP 2004), requires modulus as the mechanical material property to be used directly. Composite modulus of subgrade reaction needed in the design of rigid pavements can be estimated from the resilient moduli of geosynthetic-reinforced layer and an assumed soft subgrade modulus. These moduli therefore can be directly used in the Mechanistic-Empirical Pavement Design. Guidelines for design and construction of the working platforms using these materials and field performance are provided in related reports (WHRP Project SPR #92-00-12, WHRP Project SPR #0092-45-15, and WHRP Project SPR #0092-45-98).

2.9 REFERENCES

Chew, S. H., W. K. Wong, C. C. Ng, S. A. Tan, and G. P. Karunaratne. Strain Gauging Geotextiles Using External Gauge Attachment Method. *Grips, Clamps, Clamping Techniques, and Strain Measurement for Testing of Geosynthetics*, ASTM STP 1379, P.E. Stevenson, Eds., ASTM, West Conshohocken, PA, 2000, pp. 97-110.

Collin, J. G., T. C. Kinney, and X. Fu. Full Scale Highway Load Test of Flexible Pavement Systems with Geogrid Reinforced Base Courses. *Geosynthetics International*, Vol. 3, No. 4, 1996, pp. 537-549.

Edil, T. B., C. H. Benson, M. Bin-Shafique, B. Tanyu, W. H. Kim, and A. Senol. Field Evaluation of Construction Alternatives for Roadway Over Soft Subgrade. In *Transportation Research Record: Journal of the Transportation Research Board, No. 1786*, TRB, National Research Council, Washington, DC., 2002, pp. 36-48.

Fannin, R. J., and O. Sigurdsson. Field Observations on Stabilization of Unpaved Roads with Geosynthetics. *Journal of Geotechnical Engineering*, ASCE, Vo. 122, No. 7, 1996, pp. 544-553.

Farrag K. (1999) "Strain Gage Installation on Geosynthetics," Louisiana Transportation Research Center, Louisiana State University, Baton Rouge, LA.

Haas, R., J. Wals, and R. G. Carroll. Geogrid Reinforcement of Granular Bases in Flexible Pavements. In *Transportation Research Record: Journal of the Transportation Research Board, No. 1188*, TRB, National Research Council, Washington, DC., 1988, pp. 19-27.

Hayden, S. A., D. N. Humphrey, B. R. Christopher, K. S. Henry, and C. P. Fetten. Effectiveness of Geosynthetics for Roadway Construction in Cold Regions: Results of a Multi-Use Test Section. *Proceedings of Geosynthetics '99*, Vol. 2, Boston, MA, 1999, pp. 847-862.

Huang, Y. H. (2004) *Pavement Analysis and Design,* Prentice Hall, Inc., Englewood Cliffs, New Jersey, 2nd Edition, 775 p.

Kim, W. H. *Behavior of Geosynthetic-reinforced Aggregate Platforms Over Soft Subgrades*. Ph.D Dissertation, University of Wisconsin-Madison, Madison, Wisconsin, 2003.

Kinney, T. C., J. Abbott, and J. Schuler. Benefits of Using Geogrids for Base Reinforcement with Regard to Rutting. In *Transportation Research Record: Journal of the Transportation Research Board, No. 1611*, TRB, National Research Council, Washington, DC, 1998a, pp. 86-96.

Montanelli, F., A., Zhao, and P. Rimoldi. Geosynthetic-Reinforced Pavement System: Testing and Design. *Proceedings of Geosynthetics '97*, IFAI, Vol. 2, Long Beach, California, 1997, pp. 619-632.

Leng, J., M. A. Garb. Characteristics of Geogrid-Reinforced Aggregate Under Cyclic Load. In *Transportation Research Record: Journal of the Transportation Research Board, No. 1786*, TRB, National Research Council, Washington, DC., 2002, pp. 29-35.

Parker, F. Jr.. Estimation of Paving Materials Design from Falling Weight Deflectometer Measurements. In *Transportation Research Record: Journal of the Transportation Research Board, No. 1293*, TRB, National Research Council, Washington, DC., 1991, pp. 42-51.

Perkins, S. W. Mechanical Response of Geosynthetic-Reinforced Flexible Pavements. *Geosynthetics International*, Vol. 6, No. 5, 1999, pp. 347-382.

Perkins, S. W. *Mechanistic-Empirical Modeling and Design Model Development of Geosynthetic Reinforced Flexible Pavements*. Report No. FHWA/MN-01002/99160-1A, U.S. Department of Transportation, Federal Highway Administration, Washington, DC., 2001.

Rada, G, and M. Witcazk. Comprehensive Evaluation of Laboratory Resilient Modulus Results for Granular material. In *Transportation Research Record: Journal of the Transportation Research Board, No. 810*, TRB, National Research Council, Washington, DC., 1981, pp. 23-33.

Tanyu, B., W. H. Kim, T. B. Edil, and C. H. Benson. Comparison of Laboratory Resilient Modulus with Back-Calculated Elastic Moduli from Large-Scale Model Experiments and FWD Tests on Granular Materials. *Resilient Modulus Testing for Pavement Components*, ASTM STP 1437, G. Durham, A. Marr, and W. De Groff, eds., ASTM, West Conshohocken, PA, 2003, pp. 191-208.

Texas Transportation Institute. *MODULUS 5.0: USER's Manual*, Research Report 1987-1, Texas Transportation Institute, The Texas A&M University System, College Station, Texas, 1991.

Wisconsin. *Standard Specification for Highway and Structure Construction*, Wisconsin Department of Transportation, Madison, Wisconsin, 1996.